The Novel Use of On-Line Diagnostics for the Improved Production of Fullerenes

by

Eric Fradsham

BSc. Medicinal Chemistry, University of New Brunswick, 2015

A Thesis Submitted in Partial Fulfilment of the Requirements for the Degree of

Master of Science

in the Graduate Academic Unit of Chemical Engineering

Supervisor:	L. P. Felipe Chibante, Ph. D. Chemical Engineering
Examining Board:	Guida Bendrich, Ph.D., P.Eng. Chemical Engineering
	Brian Lowry, Ph.D., P.Eng. Chemical Engineering
	Allan Adam, PhD. Chemistry

This thesis is accepted by the Dean of Graduate Studies

THE UNIVERSITY OF NEW BRUNSWICK

April, 2019

ABSTRACT

Fullerenes, discovered in 1985, are known to form naturally in carbon-rich conditions and consequently can exist in nature and throughout the universe. Using simple characterization techniques, researchers were able to detect fullerenes in planetary nebulae. Interstellar space provides near ideal conditions to use spectroscopy, with minimal interference and low temperatures providing high signal to background, narrow peak width and well-defined energy transitions. At low pressure conditions (<1 MPa), fullerenes sublime directly to gas phase with a vapour pressure related to temperature. Fullerene vapour was generated in a tube furnace at 300^{o}C-800^{o}C under vacuum as a high temperature simulation of fullerenes in space. By monitoring fullerene abundance using infrared radiation spectroscopy (IRS) and using known thermal emission transitions, significant trends were noticed where peak intensity and area were dependent on temperature and, therefore, fullerene vapour pressure. The Applied Nano-Lab at UNB has constructed and operated a 3-phase AC plasma reactor to produce fullerenes. The oven studies under vacuum were applied to the 3-phase reactor as an on-line fullerene detector. An attempt was made to correlate mass flow rate of feedstock and volumetric flow rate of plasma gas to fullerene detection and yield.

DEDICATION

To my girlfriend Sydney Hetherington, family and friends, their constant support allowed my graduate studies to be a positive experience. To the UNB machine shop, Adon Briggs, Keith Rollins, Dwight Randall, for their valuable input to brainstorm every possible route to achieve our ultimate objective.

This project would not have been made possible without the knowledge, continuous support and drive from my supervisor, Dr. L. P. Felipe Chibante. I have learned a great deal under his supervision and consider it a great honour to be his graduate student.

I would also like to extend acknowledgments to Jun Ha Lee and Anshuman Sarawagi, without their contribution the Applied Nanotechnology Lab would not have had the success they did. Their hard work and dedication to this project is greatly appreciated.

PREFACE

This is a final thesis in partial fulfillment of the requirements of the Master of Science degree at the University of New Brunswick, Fredericton, New Brunswick.

This thesis investigates the design of the Fullerene Reactor Project by the UNB Applied Nanotechnology Lab to explore on-line spectroscopy as a diagnostic for fullerene production.

Table of Contents

List of Tables

List of Figures

List of Symbols, Nomenclature or Abbreviations

A	Amperes
AC	Alternating current
ANL@UNB	Applied Nanotechnology Lab at University of New Brunswick
C_n n ≥ 60	Fullerenes
DC	Direct current
Ful	Fullerene
ΔG	Gibb's free energy
HIV	Human immunodeficiency virus
HPLC	High pressure liquid chromatography
IR	Infrared Radiation
IRS	Infrared Radiation Spectroscopy
k	Kilo
L	Length
LII	Laser Induced Incandescence
m	Milli
µ	Micro
n	Nano
OD	Outer diameter
OES	Optical emission spectroscopy
OPV	Organic photovoltaic
PAH	Polycyclic aromatic hydrocarbon
R & D	Research and development
SLPM	Standard Litres per Minute (@ 0^oC and 760 torr)
TEM	Transmission electron microscope
1,2,4 TMB	1,2,4 Trimethylbenzene
UNB	University of New Brunswick
UV	Ultraviolet
V_{rms}	Root mean square voltage

1.0 Introduction

Carbon is a versatile atom capable of forming different structures such as graphene, diamonds, carbon nanotubes and fullerenes. This versatility arises due to the possible bonding configurations and hence electron environments. Probing the carbon environment allows monitoring of abundances and changes to the carbon material. The most recent addition to this carbon family are fullerenes, discovered in 1985 by Nobel Prize winning researchers Harold Kroto, Robert Curl and Richard Smalley at Rice University[1]. One specific form, buckminsterfullerene, also known as a buckyball, is described as a truncated icosahedron containing 60 carbon atoms, with 12 pentagons and 20 hexagons in a symmetric spherical shape as shown in **figure** 1[1]. This highly symmetric (I_h point group) pure carbon molecule, has many unique chemical and physical properties due to this symmetry. The pioneering research of Smalley and colleagues also described larger caged molecules such as C_{70}, C_{76}, C_{78}, C_{84} and more[2]. These fullerenes are able to act as semi-conductors[3], free radical oxygen scavengers[4] and lubricants[5]. The field of carbon chemistry has expanded to include fullerene derivatization which has led to a new field of organic chemistry, nano-material research and applications development.

One of the most promising applications are in photovoltaic thin films. Fullerenes readily capture photons and create an electron donor-acceptor pair, which when used with a conductive polymer will generate electricity[3] (**Figure 2**).

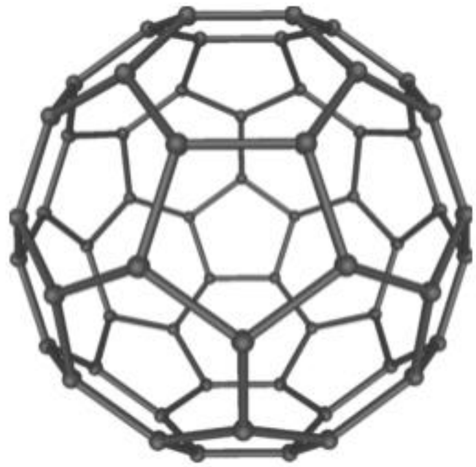

Figure 1: Buckminsterfullerene[6].

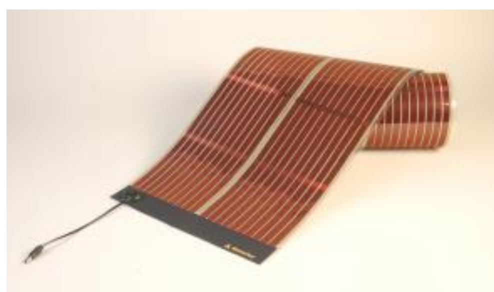

Figure 2: Flexible OPV made by Konarka.

There are many ways to produce fullerenes[13], including carbon arc[2], laser ablation of graphite[14], concentrated solar heat to ablate carbon[1], combustion[15] and plasma[13]. **Table** 1 outlines these five production methods in detail. Of these production methods, arc, laser and solar are batch processes that are not suitable to be scaled up for industrial production. The latter two methods, combustion and plasma, are continuous processes and can be scaled up accordingly. Although there are relatively high yields of fullerenes from the laser ablation of carbon material, the extremely low production rates of fullerenes and power limitations hinder this method's viability for industrial application. With combustion and plasma continuous processes, relatively high production rates have been demonstrated and have the highest potential for industrial production of fullerenes.

Table 1: Known methods to produce fullerenes[13].

Process	Principle	Continuous /Batch	Fullerene Yield (in soot) (%)	Fullerene Flow Rate (in soot) (g/h)	Upscaling
Arc	Ablation of carbon rod using an electric arc	Batch	10 (Ind.)	1	NO (UV destruction)
Laser	Ablation of carbon rod under laser beam	Batch	40 (Lab)	0.04	NO (power limitation + cost)
Solar	Ablation of carbon rod under focused sunlight	Batch	5	0.5	YES (power limitation + cost)
Combustion	In complete combustion of hydrocarbon	Continuous	5	0.5	YES (envir. + feedstock cost)
Plasma	Treatment of carbon powder by arc plasma	Continuous	5	7.5	YES (higher thermal eff. expected)

Currently, the largest manufacturer of fullerenes uses the combustion method[16]. To make fullerenes by combustion, organic solvents such as benzene are burned at low pressures (~20 Torr) in a fuel-rich environment, wherein the carbon is converted to approximately 99 wt% carbon dioxide and the remaining 1 wt% is fullerene soot. Within the soot, there is about 10 wt% fullerenes[15]. The remaining contents of the soot are mainly amorphous carbon black and some polycyclic aromatic hydrocarbons (PAH). Finally, the fullerenes are separated from the soot via extraction with organic solvents as fullerenes are soluble in these solvents making for an easy separation[20]. Due to hydrophobic[17], pi-stacking[18] and van der Waals interactions[19] between fullerenes and the aromatic organic solvents often used, there are residual solvent impurities present in the final fullerene solid that are difficult to remove even with vacuum oven drying. A continuous, large-scale operation of this process along with large scale extraction is utilized by Frontier Carbon Corp.

Three-phase plasma synthesis is a strong candidate for fullerene production for multiple reasons:

1. It can be designed for continuous processing;
2. Unconverted starting material can be recycled and reused;
3. Helium/argon gas are the only plasma gases used, no harmful greenhouse gases are produced;
4. Plasma gas can be purified, recompressed and reused to recover materials;
5. The fullerenes produced are free of any solvents used for extraction, hence are the highest purity possible[13,21].

The last reason takes advantage that fullerenes sublime, which means at the correct temperature, they go from a solid to a gas[12]. Since the fullerene sublimation temperature is low compared to the sublimation temperature of carbon black (500^{o}C vs. 4827^{o}C[23,24]), they are easily separated without the use of solvents. Solvent-free separation is a desirable process as it minimizes environmental impact, costly infrastructure (tanks, storage, pumps, distillation) and improves worker safety.

The feedstock for this process is purified carbon black and if any unconverted starting material appears in the product stream, it can be separated from the fullerene and recycled to be processed again. Ultimately, this gives 100% conversion of carbon black starting material to fullerenes. The main plasma gas used is helium. However, helium deposits worldwide are being depleted and consequently, helium is becoming increasingly expensive[22]. In the same way carbon feedstock can be recycled, the exhaust helium gas can be captured, purified, recompressed and fed back into the reactor. To increase the efficiency of the overall process, the hot helium exiting the reactor can be sent through heat exchangers to heat up the helium entering the reactor.

As will be discussed below, fullerenes are currently used in the pharmaceutical industry. High purity fullerenes are needed in this field. The solvent-free separation provides a cost-efficient process to achieve high purity fullerenes.

Compared to the combustion synthesis of fullerenes, essentially 100% conversion of starting material can be made into useful product using plasma synthesis. Fulcheri[25] had proposed a design of a 3-phase plasma reactor for this process (**Figure 3)**.

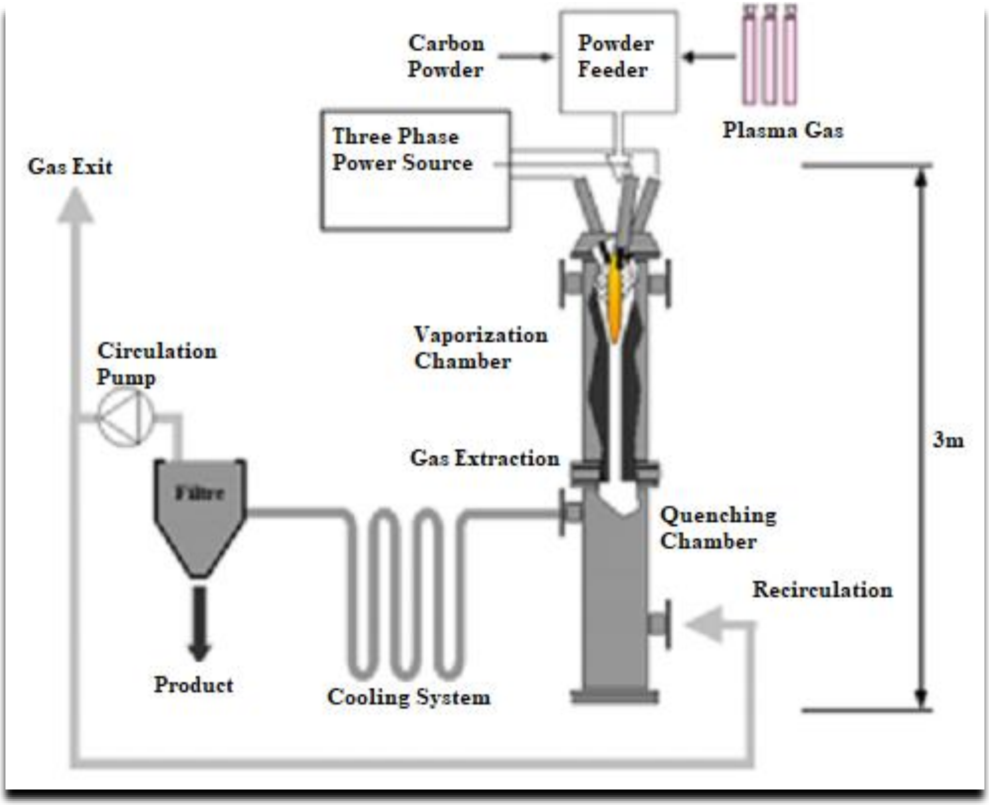

Figure 3: Proposed design for a semi-industrial 3-phase plasma reactor to produce fullerenes.[25]

To make fullerenes, enough energy to create carbon vapour is necessary. As mentioned previously, carbon sublimes at 4827°C[24]. In the hot gas phase, carbon quickly forms carbon dimers and trimers (C_2 and C_3)[26]. The excited dimers emit visible green light and these emission bands are called Swan Bands. Swan Bands cover the region from 425 nm to 625 nm[27] on the electromagnetic (EM) spectrum. Optical Emission Spectroscopy (OES) is the quantitative and qualitative observation of optical light emissions and relate to transitions between electron energy levels. OES can be used on a 3-phase plasma reactor to determine the efficiency of carbon evaporation and the amount of carbon dimers formed.

To briefly introduce spectroscopy, it is important to distinguish the different types of transitions that can occur in a molecule. The most commonly studied transitions are electronic, rotational, vibrational and rovibronic.[49] In a molecule, there are different energy levels that can be occupied by electrons. Each energy level is quantized. This means that a fixed magnitude of energy is required for an electron to transition from one energy level to the next. This is an all-or-none principle. To excite an electron from E_0 to E_1, a certain amount of energy is required. This is known as absorption. Conversely, when and electron relaxes from E_1 to E_0, the energy is emitted as EM radiation. This is known as emission. These two types of transitions are known as electronic transitions. **Figure 4** is a representation of absorption and emission of electronic transitions. Rotational and vibrational transitions are similar, but they do not involve the electrons of the molecule. Rather the atoms of the molecule move or rotate about an axis. The same principles apply, if enough incident energy is absorbed, the atoms will begin to vibrate about their equilibrium positions or rotate about an axis. Once the molecule relaxes to a lower energy level, the energy is released as EM radiation. In all these types of transitions, the absorbed or emitted radiation can be measured using spectroscopy. The quantized energy levels correspond to absorption/emission peaks on the electromagnetic spectrum[49].

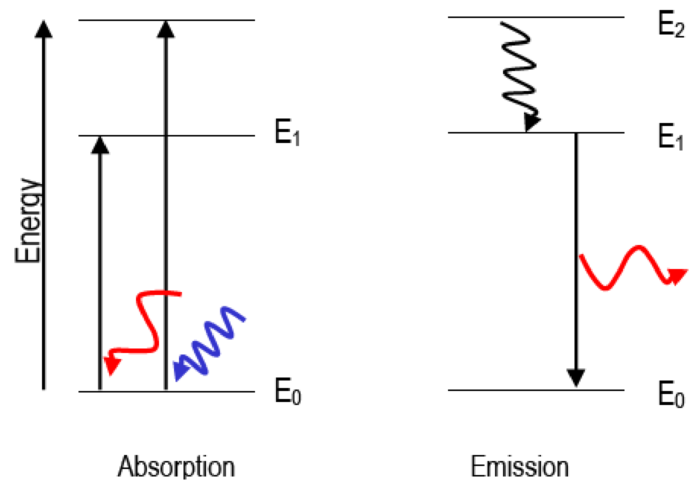

Figure 4: Diagram showing the absorption and emission of energy as electrons move through quantized energy levels[49].

Up until now, only minute yields have been published in the literature for plasma production of fullerenes. The Applied Nanotechnology Lab at UNB has been designing a 3-phase plasma reactor to produce fullerenes to overcome this issue. The use of on-line diagnostic spectroscopy on this type of reactor will be the first of its kind.

A second spectroscopic opportunity is that hot gas phase fullerenes emit infrared radiation (IR)[28]. These emissions arise from allowed transitions between different vibrational states. C_{60} emits IR at 4 distinct wavelengths of the electromagnetic spectrum. The emission bands are positioned at 7.0, 8.5, 17.4 and 18.9 microns. C_{70} has 10 distinct IR emission bands[28]. Often fullerene synthesis occurs with the formation of impurities called polyaromatic hydrocarbons (PAHs). PAHs are a common by-product of fullerene synthesis in environments containing hydrogen species. In a reaction process, water can be adsorbed onto the interior walls the vessel. At elevated temperatures, the water would desorb from the walls and react with the carbon dimers being formed. These macromolecules also emit IR when they are gases. There are specific PAH molecules that emit IR at the following wavelengths: 5.3, 5.7, 6.2, 6.4, 6.7, 7.4, 7.6, 7.8, 8.3, 8.6 and 16.4 microns[29]. Useful information regarding the chemistry and mechanism of fullerene formation can be discovered using this type of spectroscopy on a fullerene reactor.

Researchers have used this type of infrared radiation spectroscopy (IRS) to observe fullerene and PAH content in interstellar space. Carbon-rich planetary nebulae were specifically studied. Using a high-powered telescope and IRS, researchers have been able to determine the number of fullerenes, PAHs and other IR emitting species in these nebulae[30]. Space provides a near ideal environment to do spectroscopy. There is minimal interference from external thermal noise present. Specifically, cold and gaseous molecules are present. The idea to use IRS on a reactor of the kind built at the Applied Nanotechnology Lab at UNB would be novel to a plasma reactor. It would be able to probe the production rate of fullerenes and if there are any by-products being produced in real-time.

2.0 Problem Statement

The current production of fullerenes is done by a fuel-rich combustion. This is achieved by burning organic solvents using toluene for product extraction[15]. This is problematic because it is nearly impossible to obtain a pure product in a cost-efficient manner. Also, fullerenes have a relatively low solubility in toluene, approximately 2.4 g/L. This leads to product being lost in the final extraction phase of the process[20]. On the industrial scale, this low solubility would convert to over 2000 barrels of toluene used per ton of fullerenes[20]. In addition, the prolonged use and burning of organic solvents is a significant environmental hazard and has many health concerns for operators using these chemicals. Both toluene and benzene derivatives are carcinogenic compounds, and extra care must be taken by operators[31,32]. As well, the spent toluene needs to be recycled, which requires more initial capital investment. This makes it an energy intensive process[33]. Finally, the combustion method is environmentally hazardous. Most of the product of combustion is carbon dioxide gas (CO_2), and it is exhausted into the atmosphere. With Canada pushing for greener alternatives, and the idea of carbon taxation being a possibility in the near future, a production facility of this nature would be very costly[34].

The Applied Nanotechnology Lab at UNB has been designing a 3 phase AC plasma reactor to produce fullerenes, with the hopes that fullerenes can be produced commercially through this method. Plasma synthesis provides an emissions-free exhaust stream and 100% feedstock conversion through recycling. This reactor technology allows the use of spectroscopy on-line to learn and understand more about the chemistry of fullerene production. It will be very beneficial to use OES and IRS on this type of reactor.

3.0 Purpose

The purpose of this research is to use OES and IRS on a 3-phase AC plasma reactor to learn and understand the chemistry of fullerene production. The OES will be the carbon dimer detector and the IRS will be the fullerene detector.

4.0 Significance of Study

Today, 99% pure fullerene samples that are made from combustion synthesis typically cost $25,000/kg USD[35]. The Applied Nanotechnology Lab at UNB has been developing a novel 3-phase AC plasma reactor as a platform technology to produce high purity fullerenes, solvent-free, at a low cost.

To produce fullerenes in this reactor, a preheated and aerosolized carbon black feedstock is propelled by helium carrier gas into a region of hot 3-phase AC plasma. The energy of the plasma is enough to ablate and sublime the carbon feedstock. Once in the gaseous form, the carbon immediately forms dimers. If the C_2 dimers have enough residence time, the fullerene growth pathway begins when they bind to one another and form spherical shaped fullerenes.[36]. Once formed, the fullerenes are quenched and collected on a filter in a collection chamber up-stream. Up until now, the reactor has only produced a maximum yield of 5% on the rare occasion, with minimal collection.

This research will mainly focus on the dynamics of the chemistry going on up-stream of the plasma region. By using spectroscopy, information regarding species identity and concentration can be determined after the carbon feedstock has been evaporated. With this information, design and process operating parameters can be changed to achieve the highest conversion of feedstock to fullerenes possible.

This project will mainly focus on the characterization of chemical compounds that are present inside the reactor, while the reaction is taking place, to help predict the causes of high or low fullerene yields. This information will help determine whether all the fullerenes being made are being collected, or if there are losses between fullerene formation and the collection stage. Accordingly, design and process operation changes can be made. This type of study has never been published in the literature and will be mainly a proof of concept, or a preliminary type of experiment to determine whether spectroscopy is feasible as an on-line detector. This would also give information regarding fullerene formation chemistry, and it would conclude whether potential by-products could be formed from this process. Considering this, design changes can then be made to optimize fullerene production. The use of both OES and IRS at different points along the reactor will allow for the observation at the beginning, growth and final stages of fullerene formation, and where they take place in the reactor. The OES will provide relative temperatures of plasma gases. With the resulting temperature given from the OES and the power supplied to the plasma torch, an assumption can then be made to determine the efficiency of carbon evaporation within the plasma.

5.0 Literature Review

To gain an understanding of how to design a reactor with the ability to have on-line spectroscopy, an in-depth literature search of all fullerene synthetic methods, as well as how fullerenes are formed, was necessary.

5.1 Manufacturing of Fullerenes

Since fullerenes were discovered in 1985, it is apparent that they have numerous applications, including solar photovoltaic applications, lubricants, fuel additives, cosmetics and pharmaceutical applications. **Table 2** describes some conventional fullerene synthesis methods.

Table 2: Different manufacturing methods for fullerenes[13,37].

Process	Principle	Pressure (torr)	Mass Flow Rate (soot) (g/h)	Fullerene Yield (in soot) (%)
Arc	Carbon rod ablation by electric arc	75-375	10	10 (Industrial)
Laser	Carbon rod ablation by laser beam	75-375	0.1	40 (Lab)
Solar	Carbon rod ablation by focused sunlight	75-375	20	5
Combustion	Incomplete combustion of hydrocarbon	37.5	10	10-20
Plasma	Carbon powder treatment by arc plasma	750	150	5 (pilot)

Because there are no efficient large-scale synthesis methods currently available, fullerenes are extremely expensive. Some of the current, novel and well-known methods to produce fullerenes are laser, arc, solar and combustion, developed by Kroto[36], Kratschmer[37], Guillard and Howard[40], respectively. These techniques would seem viable, however, they require unique reaction conditions, such as sub-atmospheric pressures and high currents. Power limitations prevent some of these methods from being scaled up to large-scale synthesis.

5.1.1 Carbon Arc Generation of Fullerenes

Based on Krätschmer and Huffman's first macroscopic production of C_{60}, a group of researchers designed a synthesis method to produce fullerene mixtures on the order of gram quantities per day. Using a contact-arc C_{60} generator shown in **Figure 5**[38], a fullerene mixture was created. A 6 mm graphite rod (sharpened at one end for precise contact area) was held in contact with a graphite disk by slight spring pressure. The surrounding copper walls were water cooled for efficient collection of carbon vapour condensate. The chamber was evacuated to 10^{-6} torr to remove any atmospheric gases, and the pressure was raised to and maintained at 100 torr by bleeding helium gas at a rate of 1 sccm in conjunction with a small rotary pump. A strong current of 100-200 A at 10-20 V_{rms} was applied across the graphite rod to generate the arc. This arc was hot enough to evaporate the graphite and generate carbon vapour. From this carbon vapour, fullerenes were formed.

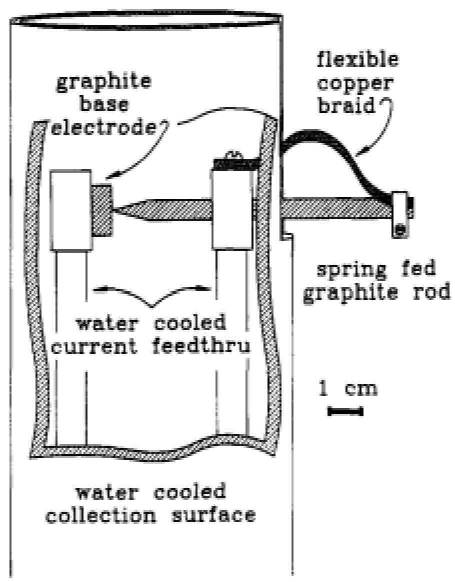

Figure 5: C_{60} generator, schematic representation of graphite rod contact-arc.[38]

Soot-like material was generated in a volcano eruption fashion, travelling upwards from the arc. After a few hours of operation, approximately 10 grams of soot material was collected on the water-cooled walls by scrapping it off. The collected soot was removed and placed in the thimble of a Soxhlet extractor (**Figure 6**[39]), and after 3 hours of extraction in boiling toluene, a reddish-brown solution remained[37]. The solution was placed in a rotavapor distillation set-up where toluene was evaporated, leaving behind a dark solid. This solid yielded both C_{60} and C_{70} in significant quantities. The analytic measurement used was Knudsen effusion mass spectroscopy[12,39]. However, only one gram quantities per day were produced. In addition, the carbon arc generation of fullerenes is a batch process, and in order to collect the final product, the operation must be shut down. On an industrial scale, this causes major issues in lost time that could be used for fullerene synthesis instead.

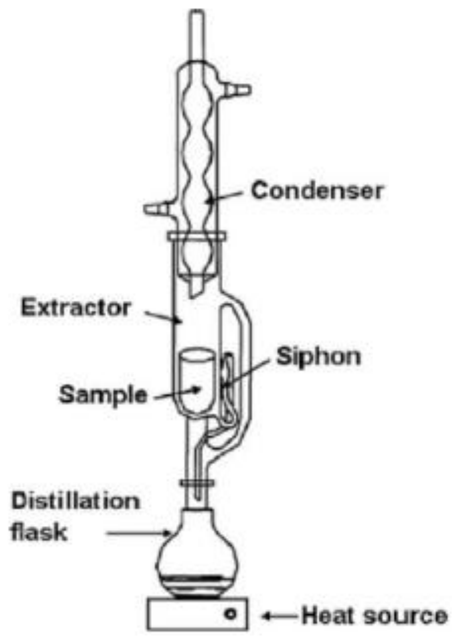

Figure 6: Schematic diagram of a Soxhlet Extractor.[40]

5.1.2 Formation of Fullerenes by Incomplete Combustion of hydrocarbons

An understanding of all potential manufacturing techniques is important for the study of fullerenes. Whether or not spectroscopy can be done on the incomplete combustion of hydrocarbons could be answered by studying how the process works. Even though the combustion method has many drawbacks, as described previously, it is currently the market leading producer of fullerenes today. Up until the discovery of fullerene production by the combustion of hydrocarbons, it was stated that an environment lacking oxygen and hydrogen was needed. Therefore, the arc discharge method dominated fullerene synthesis. It wasn't until Gerhardt-Loffler-Homann discovered that fullerenes were present in flames produced by burning hydrocarbons, that the combustion of organic solvents was used to synthesize fullernes[41]. In 1991, fullerenes were first extracted from a flaming soot.[15] This has led to intense research in the area of combustion and pyrolysis of hydrocarbons for the production of fullerenes.

There are many potential designs for the combustion torch, and a sample of one design is shown in **Figure 7**.[41] Although there are many different designs, the only two that have been optimized are the premixed flame and laminar jet diffusion flame torches. For the premixed flame torch, hydrocarbon and gas are mixed and sent through a water-cooled burner to be combusted in a sub-atmospheric chamber. CO_2 and soot are produced, and the condensable soot is collected on water-cooled collector plates. Researchers have adjusted key parameters such as the carbon/oxygen (C/O) ratio. It has been found that in higher C/O ratios, a higher relative percent of soot is generated. In turn, a higher concentration of fullerenes is also generated. Some key results have been seen through this combustion technique. First, the mole ratio of C_{70}/C_{60} ranges from 0.26-8.8. Second, undesirable by-products are formed, such as $C_{60}O$, $C_{70}O$, $C_{60}H_2$, $C_{60}CH_4$ and $C_{70}H_2$. Lastly, isomers of C_{60} and C_{70} have been detected in the final product.

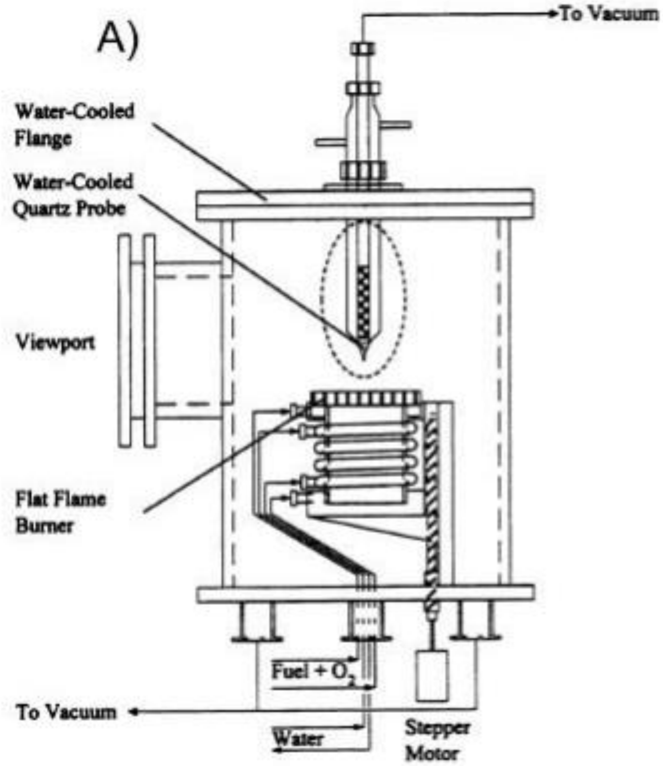

Figure 7: This figure shows a premixed combustion chamber whit a burner and microprobe sampling system to produce fullerenes.[41]

5.1.3 Fullerene Production from a 3-phase AC Plasma Reactor

The use of 3-phase plasma in a reactor can also be used as a potential method to produce fullerenes. With combustion being the leading producer of fullerenes, the main goal is to produce them on the industrial scale. However, there are major drawbacks, including the environmental impact of CO_2 exhausted to the atmosphere. Because of this, in 1993, it was proposed that fullerenes can be made using a 3-phase AC plasma to evaporate and condense carbon vapour in an entrained flow[21]. This type of reactor uses the heat generated from a helium or argon plasma (ionized gas) to vapourize carbon and produce fullerenes. Researchers explored the effect of many different parameters on yield. To no surprise, researchers concluded that there was a relationship between internal reactor pressure and fullerene yield. It was determined that fullerene yield at low pressures was higher compared to atmospheric data[42]. AC plasma provides a stable plasma that is energetically favourable. From these results, it was concluded that AC plasma can be a viable technology for fullerene production.

Fulcheri *et al.* designed and tested a fullerene reactor under multiple conditions to verify its validity as a production method for fullerenes. **Figure 8** is a schematic representation of a pilot scale plasma reactor[21]. The plasma was generated by an AC arc across 3 electrodes connected in different phases. By sending ionizable gas through the electric arc, it generates plasma. Helium or argon gas is typically used. The ionized gas created very strong electric fields, high temperatures, turbulent flow and sufficient energy to evaporate materials that have high boiling/sublimation temperatures. The carbon was introduced to the plasma region as an aerosol in the helium carrier/plasma gas. The plasma treated fullerene soot was collected in chamber with a filter.

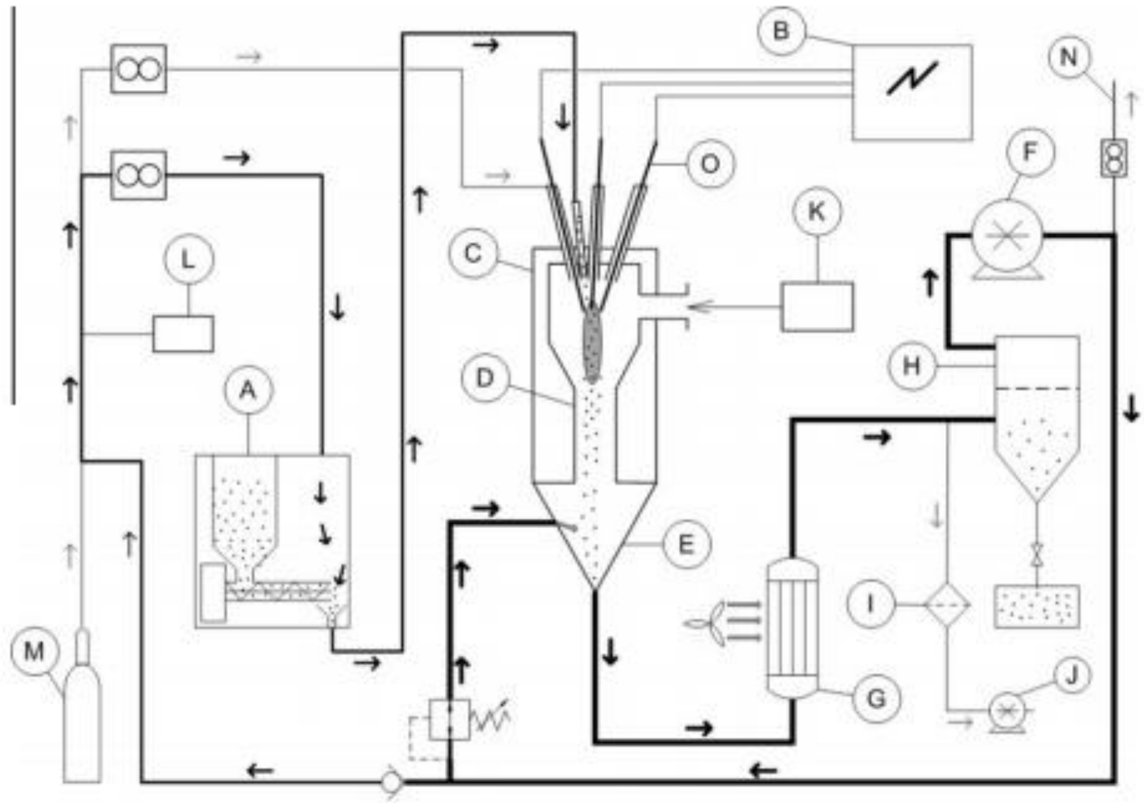

Figure 8: General scheme of fullerene production by the 3-phase AC plasma method. Black arrows indicate carbon flow and grey arrows indicate gas flow[21].

The key parameters that were tested in this reactor are outlined in **Table 3**. Research found that carbon type does have a huge impact on yield. Fulcheri *et al.* discovered that acetylene black feedstock provided the highest yield. Carbon purity and particle surface area also have a significant effect on yield. If impurities such as hydrogen, oxygen or nitrogen are present, a lower yield was observed because carbon radicals bind with these atoms due to the increased collision frequency at elevated temperatures. In addition, particle surface area plays an important role because the higher the surface area, the greater the evaporation efficiency. If more carbon per unit volume is being exposed to heat, more carbon will evaporate. The acetylene black used had the highest surface area of the 3 tested and was ranked 2nd for purity at 99.5% pure carbon. With continuous feed of the carbon feedstock, Fulcheri *et al*. achieved a maximum yield of 4.5 wt% fullerenes[21]. Finally, they were able to obtain 17 g h^{-1} of fullerite (C_{60}+C_{70} and C_{70+n}) from a carbon feed rate of 480 g h^{-1}. All unreacted carbon can be separated from fullerite and sent back through the reactor as recycled feedstock. This results in a 100% conversion from carbon black to fullerite over time. Due to the helium shortage worldwide and increased cost, some researchers are collecting the helium exhaust gas and using purifiers and compressors to recycle the helium.

Table 3: Main operation conditions tested on a 3-phase AC plasma reactor[21].

Main Operating Conditions	
Carbon Precursor	Y50 A, E 250, KS 4
Gas Flow Rate	10, 15, 20, 25, 30, 35 Nm^3 h^{-1}
Carbon Flow Rate	200, 300, 400, 500, 600 g h^{-1}
Recirculation Flow	200 m^3 h^{-1} ± 10% @ STP
Voltage	80 V ± 10%
Current	220A ± 10%
cos ϕ	0.62 ± 10%
Plasma Power	18.9kW ± 20%

Y50 A is an acetylene black, this feedstock is produced from pyrolyzing acetylene gas. E 250 is a graphitized carbon black, it has high structure, but low surface area. Finally, KS

4 is an amorphous carbon black. The cos ϕ refers to the phase separation. In 3-phase power, the wave function is out-of-phase by a factor of ϕ[21].

5.2 Mechanism for Fullerene Formation

5.2.1 The "Party line"

While studying the spectroscopy of carbon dimers and fullerenes, an understanding of how these molecules are formed is important. A clear reaction mechanism for the formation of fullerenes from carbon vapour is highly debated among researchers. Therefore, a definitive answer is not yet known.

After the discovery of fullerenes, Richard Smalley and his research group made efforts to decipher a reaction pathway. In this pathway, dangling bonds on graphitic sheets of carbon give carbon atoms the ability to interact with one another, having an effective valence of 3[26]. To study how the fullerenes grew, a very intricate reaction vessel was built. Focusing a Nd:YAG laser at 532 nm onto a rotating/translating disk of graphite created a hot plasma of carbon vapour 10,000^{o}C[26]. Then, a pulse of helium gas was used to cool the carbon vapour. Controlled gas flow and flow geometry allowed for annealing of the carbon. This allowed for manipulation of the residence time of the carbon vapour in the reaction zone of the reactor[26]. To study the carbon clusters and fullerenes generated, time-of-flight (TOF) mass spectrometry and laser spectroscopy were used.

It was found that carbon clusters only grew in even numbers after at least 26 carbons were attached. Growth from C_2 to C_{25} was considered a "forbidden zone", in which very little signal was given[43]. From the literature and results obtained in this study, Richard Smalley proposed a mechanistic pathway. He called it the "party line"[42]. In this mechanism, linear chains of carbon bind together to form longer chains. Once enough carbons have been added, they can form monocyclic rings. These rings then bind with other carbon dimers and radicals to form C_{25} continuing to C_{32}[42]. Lower carbon content clusters contain many dangling bonds, which are very high in energy. These high energy clusters will not exist in a carbon rich environment if they are able to grow to a more stable carbon cluster. These open graphitic sheets rearrange to incorporate pentagons into their pattern. As pentagons form, the sheet begins to curve[42]. It was found that pentagons do not form adjacent to one another. This would cause a sharp corner in the structure, which is energetically unfavorable. As more C_2 dimers are added and the formation of pentagons continues, a small fraction grows into stable fullerenes. In high H_2 content environments or fuel rich flames, the carbon cluster continues to grow uncontrollably into high carbon content clusters, such as C_{100} and greater[42].

5.2.2 The Pentagon Road

The pentagon road mechanism is similar to the party line, however, the key process parameter is annealing[36]. Thermodynamically, fullerenes are most stable when they have the maximum number of pentagons. A standard graphitic sheet of carbon contains only hexagons. As soon as pentagons are added, the sheet begins to curl. Pentagons are never adjacent as this would create high energy corners[36]. By adjusting the parameters such as gas flow rate and flow geometry, it allows the carbon vapour to have enough time to anneal into fullerenes. This annealing process can be made possible by expansion cooling. As gases expand from a smaller volume to a larger volume, there is a change in temperature as per the Ideal Gas Law. The larger the change in volume, the greater the temperature change[44]. By altering the pressure of the reactor, one has some control over the fullerene growth rate, which allows for the control over the annealing process[26]. Many researchers believed that the amount of carbon vaporized was the key parameter. However, for the pentagon road mechanism, it is the conditions concerned with the condensation of carbon vapour that are important[26]. Ultimately, by lowering the pressure, control can be obtained of the migration rate of carbon away from the heat source. This allows for control over how fast the carbon vapour will begin to anneal.

To further emphasize the temperature dependence on fullerene formation, **Figure 9** demonstrates how different carbon cluster products can be formed at uncontrolled temperatures. To further simplify the diagram, it is important to imagine that each new structure is formed by C_2 dimers adding to the pre-existing structure. First, C_2 adds to one another to form linear chains. Once approximately 10 carbon atoms are bound, monocyclic ring structures begin to form. Under controlled temperature conditions and subsequent addition of C_2 dimers, multi-cyclic systems begin to form. These multi-ring structures with the integration of pentagons begin to curve, such that cage structures form. At about 50 carbon atoms, there is a strong equilibrium favouring a closed cage structure, instead of an open cage structure. This is mainly due to the high energy dangling bonds present on an open cage structure. Finally, with addition of more C_2 dimers, stable fullerenes are formed[45]. The experiments performed to determine this outcome also discovered that fullerenes can be formed on a picosecond time scale[45]. It is critical that the temperature is controlled in this process. As more C_2 dimers are added, and new structures are formed, the temperature trends downward. If the temperature of the system remains hot (i.e. sublimation temperature of carbon, >4287^{o}C), then chaotic 3-dimensional structures would form (i.e. amorphous carbon)[45]. If the temperature is controlled, for example by controlled annealing, one could successfully form fullerenes by the continuous addition of C_2 dimers.

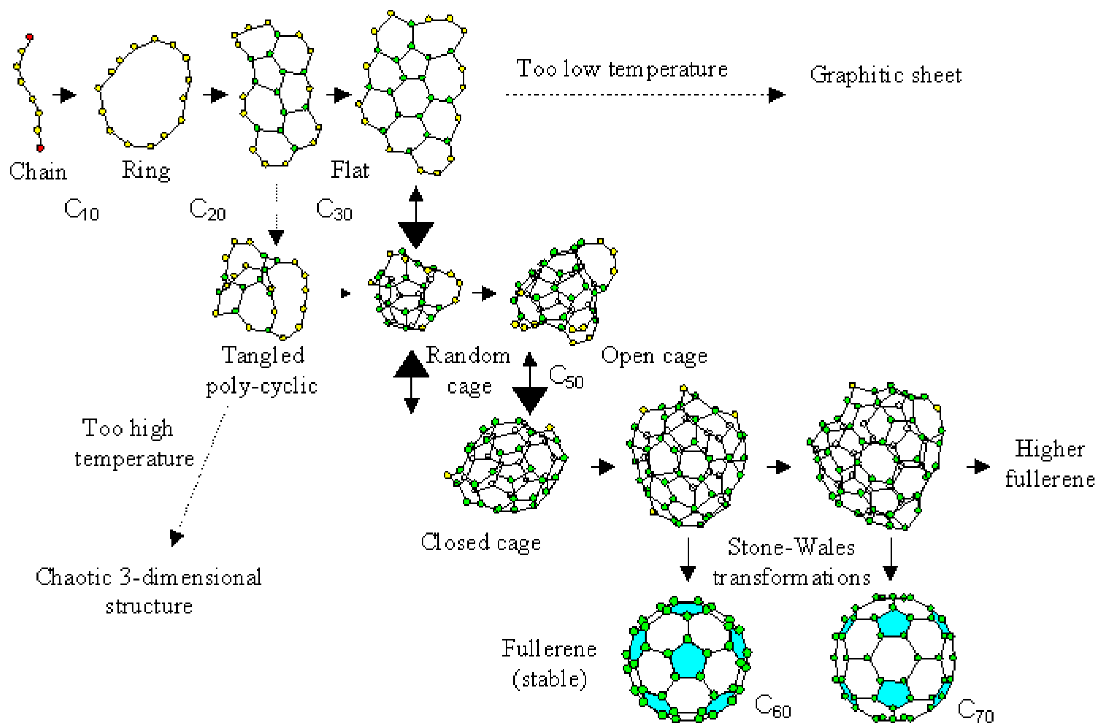

Figure 9: C_2 addition mechanism for the growth of fullerenes. Temperature dependence also illustrated[45].

5.3 Spectroscopic Techniques for Fullerene Analysis

5.3.1 Optical Emission Spectroscopy on an RF Thermal Plasma Reactor

It is well known that carbon vapour plasma quickly forms carbon radicals in the form of dimers and trimers (C_2 and C_3). When the dimers are formed, they emit green light and can be measured using spectroscopy. Green emission falls within the visible light region of the electromagnetic spectrum. More specifically, the Swan bands of C_2 emission occur between 425 nm and 625 nm[27]. A spectrum of C_2 emission can give insight about the chemistry taking place. Peak position indicates which transition is occurring. Whether *$\Delta v=0$, 1 or -1*, peak intensity and area indicate the relative concentration of the species, and peak width at half max indicates the rotational temperature of the dimer[46]. Researchers designed a radio frequency (RF) thermal plasma reactor to produce fullerenes, and they used OES to study the carbon vapour produced[47]. These researchers discovered that gas velocity, maximum temperature, volume of plasma flame and carbon concentration in the plasma all affect fullerene yield. Both maximum temperature and carbon concentration in the plasma were calculated using OES[47]. For the highest thermal efficiency, helium gas was used as the plasma gas because of its high thermal conductivity relative to argon[48]. From previous research, it is known that fullerenes require an inert environment at temperatures greater than 2000 degrees Kelvin to grow[45]. The observation of an emission signal representing a CN was not intuitive because inert conditions are necessary for the formation of fullerenes. Nitrogen gas (N_2), is considered an inert gas. However, at the elevated temperatures considered here, there is enough energy to dissociate the nitrogen triple bond (bond dissociation energy of N≡N is 945.33 kJ/mol)[47]. Therefore, a comparison between C_2 and CN was necessary. It was found that the only time the $I(C_2)/I(CN)$ ratio decreased was when there was an increase in the argon sheath gas flow rate[47]. It was stated that the nitrogen contributing to the CN emission band was due to the nitrogen present in the 99.995% pure argon. The researchers used a Boltzmann-plot to determine the rotational temperature of C_2 and found it to vary from 4800-5000 degrees Kelvin[47]. Finally, it was discovered that fullerene yield plateaued at 20%. Perhaps there was something else occurring that their spectroscopic techniques could not detect. **Figure 10** is an optical emission spectrum obtained from experiments performed on the RF thermal plasma reactor.

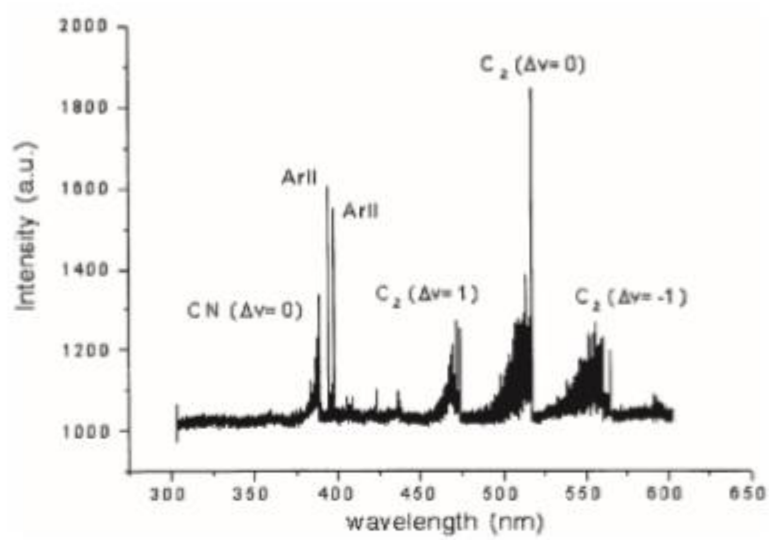

Figure 10: Sample Optical Emission Spectrum from an RF thermal plasma reactor[47].

From the above spectrum, the presence of C_2 in the RF thermal plasma reactor was detected. They also stated that an argon plasma gas was used, the emission of argon was seen at a wavelength of approximately 390 nm. Finally, the presence of a nitrogen impurity was also detected as CN. It had an emission band at 389 nm[47].

5.3.2 Using Infrared Radiation Spectroscopy to Detect Fullerenes in Space

Richard Smalley and his colleagues believed that fullerenes were made in space. It wasn't until a group of researchers teamed up with space scientists using powerful telescopes and IRS, that neutral fullerenes were observed in planetary nebulae[29]. C_{60} is the most symmetric known molecule. Using the 3N-6[49] rule for vibrational degrees of freedom (DOF), C_{60} has 174 DOF. However, the icosahedral symmetry of this molecule leads to multiple degenerate frequencies. Therefore, only 46 frequencies are expected for C_{60}. Of the 46 frequencies, 10 are Raman active and 4 are IR active[50]. The IR active modes of C_{60} are located at 7.0 µm, 8.5 µm, 17.4 µm and 18.9 µm[30]. The remaining 32 frequencies are neither IR active, or Raman active.

Where are fullerenes formed in space? That is a question that has yet to be answered. Some believe that they can be found in carbon rich stars. Others believe that hydrogenated amorphous carbon grains decompose into fullerenes and PAHs. This is caused by interstellar shock which is a process that occurs in the ejecta of a type II supernova. Some scientists also believe that fullerenes are a product of cold interstellar gas chemistry[29]. According to a group of researchers who were studying nebula NGC 7023, it was found that 0.1%-0.6% of interstellar carbon is C_{60} and that 50% of the mass of stable fullerenes is C_{60}[29]. The peaks observed while studying NGC 7023 were consistent with their laboratory experiments of UV-excited-gas-phase C_{60}. A substantial amount of PAH was found in the nebula as well. It was observed that PAH emission peaks were near some of the C_{60} emission peaks. These emission signals blended together. In PAH rich areas of space, the PAH emissions at 8.6 µm and 16.4 µm, blended with C_{60}'s 8.5 µm and 17.4 µm peaks[29]. Finally, it was concluded that the emission solely due to C_{60} (18.9µm), had a different spatial distribution than the emission of PAH[29]. This meant that C_{60} and PAH were in different locations relative to the hot central star. C_{60} was closer to the central star than PAH, and an emission of H_2 was seen even further away. **Figure 11** is an IR emission spectrum from a different research group studying planetary nebula Tc1.

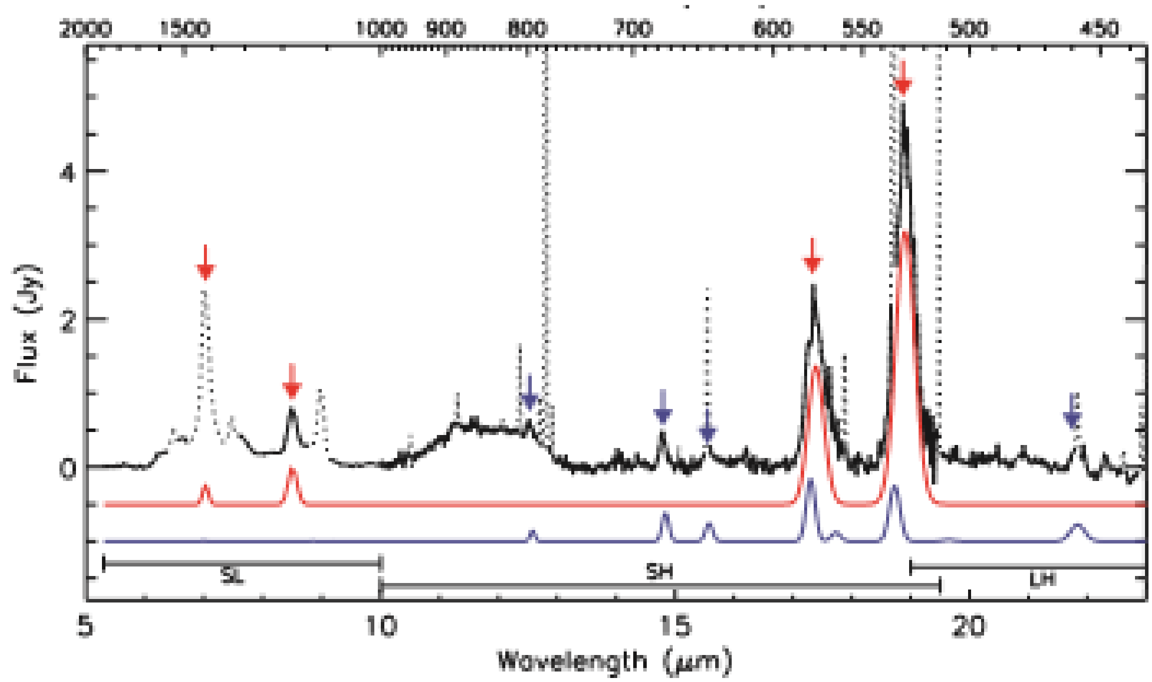

Figure 11: IR Emission Spectrum from planetary nebula Tc1. C_{60} peaks are indicated by the red line and red arrows. C_{70} peaks are indicated by the blue line and blue arrows[30].

The above spectrum clearly depicts the presence of C_{60} and C_{70} in the planetary nebula. It can also be seen that at the emission band at 17.4 and 18.9 microns, there is contributions by C_{60} and C_{70}. This can be seen by the shoulder on the peak. Finally, it can be concluded that there are PAHs present in this planetary nebula due to the very broad peak ranging from 11-13 microns[30].

6.0 Research Questions

This research explores whether the use of spectroscopy can be used on a running 3-phase AC plasma reactor to detect fullerene formation. The main question regarding this research is if an IRS can accurately detect the number of fullerenes emitting IR.

To answer the main question, some minor questions must be answered along the way. Does peak intensity increase with increased fullerene content in a linear relationship? Can these trends be seen in a reactor with a lot of signal interference (carbon black, red hot background graphite)? Which part of the reactor will the "fullerene detector" be located? Can the IR spectrometer obtain on-line results?

7.0 Hypothesis

Since the only atoms introduced into the reactor are carbon and helium, there should only be IR signals from fullerenes and optical emission signals from C_2. However, with the constant opening of the reactor to clean the torch area, some atmospheric air may continuously diffuse into the reactor. Nonetheless, the reactor, carbon feeder and carbon feedstock are constantly purged with argon or helium. I hypothesize that CN and CO peaks will be seen on the OES, and that PAH signals will be detected on the IRS. Their intensities should only be small relative to C_2 and C_{60}.

Since the yield of fullerenes produced is dependent on the mass flow rate of carbon and helium into the plasma, and therefore carbon concentration in the plasma, I hypothesize that as carbon concentration increases, fullerene content will also increase. As more carbon atoms per liter of helium are evaporating, more fullerenes per liter of helium will be produced. As more carbon is being evaporated, an increase in the C_2 signal intensity and peak area in the Swan band region will be observed. An increase in intensity and peak area of the four infrared active modes of C_{60} will be seen also. The research groups studying fullerene content in space had ease identifying accurate concentrations of fullerenes in the respective planetary nebulae. However, I hypothesize it will be more difficult to do this on a running reactor with entrained flow. When considering the environment of outer space, there is minimal interference while performing spectroscopy. Particles are far apart from each other, and they do not absorb radiation emitted from other fullerene molecules before reaching the spectrometer. This is relevant because as every particle emits IR, every particle absorbs IR. If a portion of an IR signal is absorbed by a free-floating particle before reaching the spectrometer, the information received by the spectrometer is not indicative of the source. For IR emission on a plasma reactor set-up, there will be many particles interfering with the emission signal. As unreacted carbon black passes through the path of IR from an emitting fullerene, the signal received from the spectrometer will be inaccurate. Due to this, trends from the reactor testing fullerene content will be difficult to analyze.

However, by having an *in situ* sublimator, results can be analyzed more accurately. In the sublimator, gaseous fullerenes emitting IR will not interfere with aerosolized carbon black. The IR emission signal will be accurate because of this. With a small relative concentration of fullerenes in the sublimator, and the soot taken directly from the previous experiment, there should be an increase in fullerene emission intensity and peak area. This is because there is an increased number of fullerenes in the soot.

8.0 Methodology

To mimic the emission profile for fullerenes in space, fullerene IR emission was first tested on a tube furnace/offline sublimator. Fullerenes were under vacuum at varying temperatures to determine the intensity and area of the emission signals. After the data was collected and analyzed from the tube furnace experiments, the IRS was placed in front of a potassium bromide (KBr) viewport on a 3-phase AC plasma reactor to test for fullerene emission. The Applied Nanotechnology Lab at UNB developed and optimized a 3-phase AC plasma reactor to produce fullerenes. Intensive designs, preliminary experimentation, materials science research and trial and error tests were done to develop this reactor and have prepared it for experimental use.

Construction and operation of the reactor along with addition of additional diagnostics were done in room B24-C in Head Hall at UNB. The reactor and other ancillary pieces of equipment are shown in **Figure 12**. Preliminary experiments and data analysis for fullerene yields were done in Enterprise Building 2 prior to relocation.

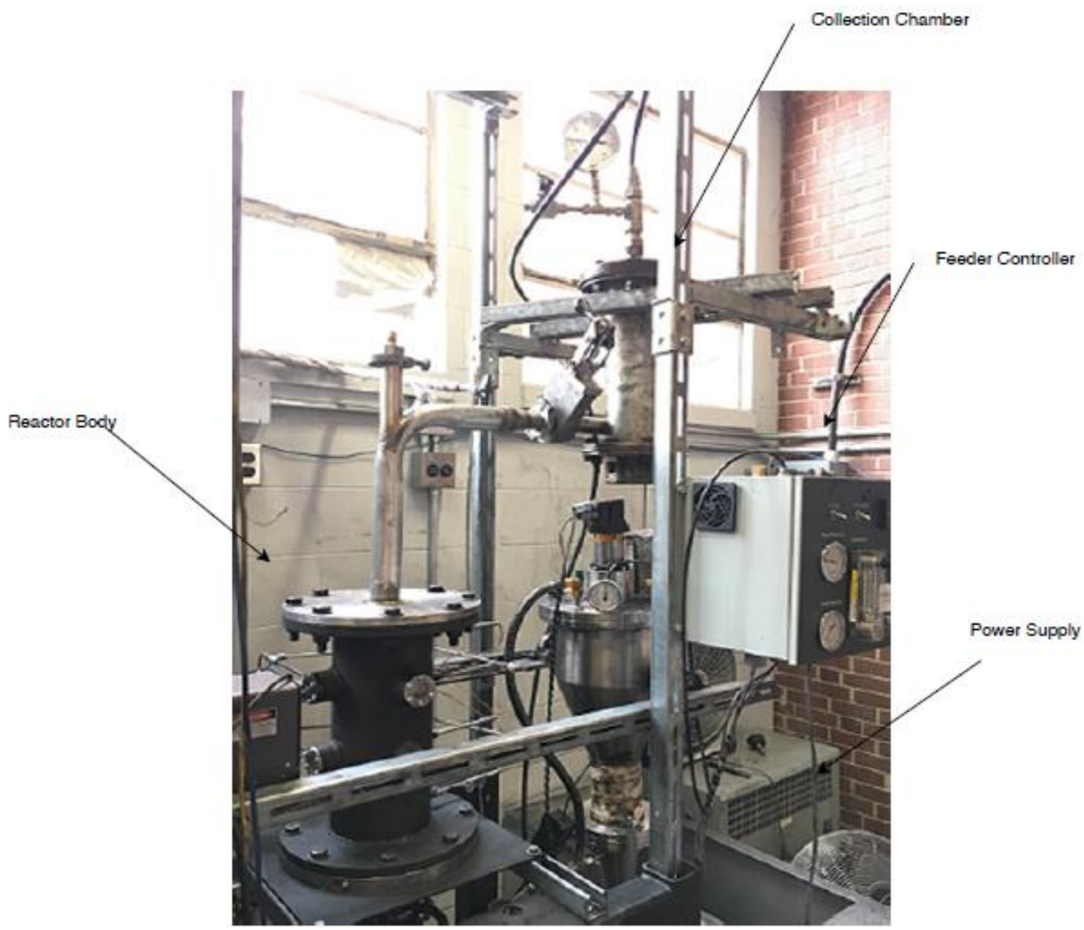

Figure 12: Applied Nanotechnology Lab's fullerene reactor in Head Hall at the University of New Brunswick.

8.1 Reactor Description

The first couple years of the project were devoted to the design and optimization of a 3-phase AC plasma reactor with several generations of design worked on. Due to the power supply limitations at Enterprise Building 2, scale up of the reactor was not possible. The reactor power sources used at Enterprise Building 2 had a duty cycle of two minutes, meaning that after two minutes of operation, the power supply had to be turned off to cool.

This was not long enough to produce fullerenes continuously. It was decided that the 3-phase 600 V and 100 A power available at Head Hall would be more suitable for the pilot scale reactor.

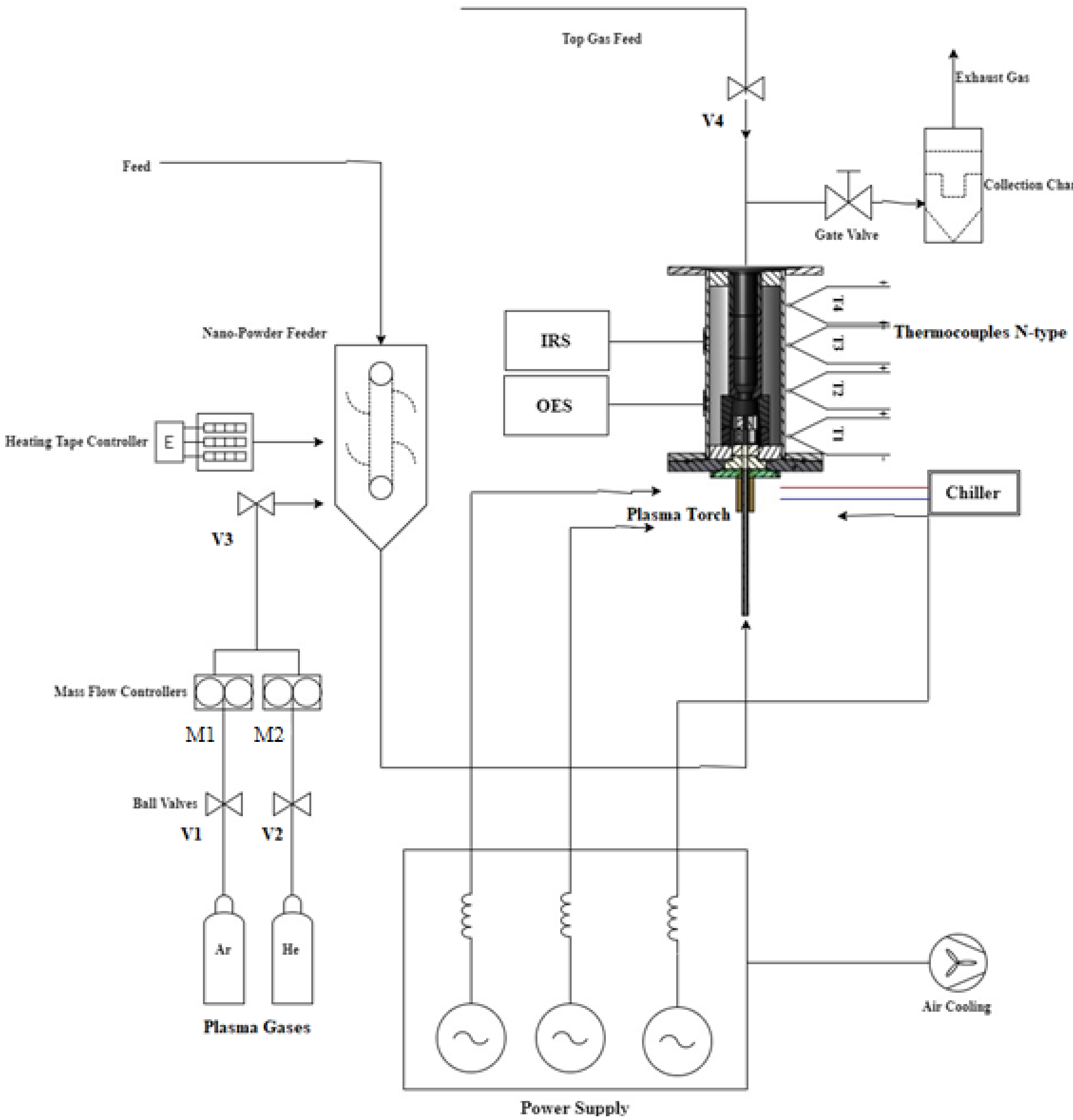

Figure 13: Schematic of the 3-phase AC plasma fullerene reactor.

Each part of the schematic diagram in **Figure 13** will be described in detail throughout this section.

8.1.1 Power Supply

Due to power limitations during the preliminary experiments at Enterprise building 2 at UNB, the Applied Nanotechnology Lab decided to relocate to Head Hall. At this facility, 600 V and 3-phase power was readily available. The 600 V, 3-phase power travels through a step-down transformer, stepping the voltage down from 600 V phase-to-phase to 240 V phase-to-phase. At this voltage, the current would reach upwards of 280 A. Internal structures of the reactor such as graphite electrodes, the graphite shell and the ceramic insulation undergo thermal degradation at this power. To overcome this potential issue, each phase was sent to an inductor at 4.2 millihenries (mH), dropping the current to approximately 180 A. The inductance was determined through trial and error using an LCR meter (inductance, capacitance and resistance) and testing the voltage/amperage at a pseudo-plasma torch set-up. From the inductors, each phase was connected to a separate electrode at the torch housing inside the reactor. Cooling fans were mounted on the outside casing of the transformer and inductors, to allow for forced air convection in order to cool the power supply during prolonged experiments. A power meter, which measured voltage, current, phase angle and total power was connected to the power supplying the transformer. Calculations were performed to determine the amount of energy used to power the reactor for each experiment. Voltage and current were measured at the torch using a handheld multi-meter to determine the power after the inductors.

8.1.2 Water Cooling

To ensure the brass electrodes did not melt inside the reactor, a Polyscience LS51 benchtop chiller was used to constantly flow cold water through the electrodes on the plasma torch. It was crucial to prevent the brass from melting. If the brass melted, water inside the electrodes would rush into the reactor and immediately form steam. This would be very dangerous considering the power of 6 kilowatts (kW) being used in the reactor. To maintain a constant water flow to the torch, manual flow meters were used. The flow was consistent at 0.757 litres per minute (LPM), with the chiller set to 10^{o}C. A pressure gauge was attached to the water-cooling manifold to monitor any instant changes in pressure, which could indicate steam formation inside the water-cooling lines. N-type thermocouples were incorporated at the outflow lines of each electrode to monitor the temperature coming out of the electrodes. Temperature and data acquisition was monitored using LabView software.

8.1.3 Powder Feeder

A nano-powder feeder was used to store and supply carbon black nano-powder to the reactor. The PFR400 Fine Powder Feeding System was purchased from Tekna Plasma Systems Inc. The powder feeder was wrapped with electric heating tape and maintained at 250^{o}C with argon constantly flowing through the inside of the feeder. This was to ensure any moisture or atmospheric gasses adsorbed to the carbon black were removed.

8.1.4 Gas Handling

Argon and helium plasma gas were connected to a gas handling manifold built by the members of the Applied Nanotechnology Lab. Gas flow was controlled using mass flow controllers (MFCs) from MKS Instruments, Inc. Two MFCs with a max flow of 25 standard liters per minute (SLPM) were connected to each of the two gases respectively (labelled as M1 and M2 to control each gas). From here, the hoses converged and connected into one hose that was split using a t-fitting. After the t-fitting was three more MFCs, two with max flows of 50 SLPM, and one with a max flow of 25 SLPM. These were used as valves to direct and control the amount of gas flowing to different parts of the reactor. A MFC directed gas flow to the top of the reactor, as shown in **Figure 13**, and a separate MFC directed gas flow to the nano-powder feeder. From the nano-powder feeder, the gas collected aerosolized the carbon black and propelled it through the bottom of the plasma torch and into the reactor. Gas flow through the top of the reactor was necessary because when removing the torch for cleaning, constant flow from the top helped minimize the diffusion of atmospheric gases into the reactor. Finally, the smaller MFC controlled the small amount of gas travelling to the viewports. Gas flow to the viewports reduced the carbon from clogging the viewports. The MFCs were powered by a connection to a control box, which controlled the position of the main valve. This acted as a switch for the MFC by opening and closing the MFC. Maximum flow rates for each MFC were set using the CCR control box. The gas flow rate was controlled using MKS software found on the provider’s website. The software allowed for the selection of which gas each MFC controlled, and the flow rate and the operating pressure for the gas was chosen. By following this method, accurate flow rates for the gases were detected. The software and the MFCs were pre-calibrated with correction values for each type of gas used.

8.1.5 Online Diagnostics

OES and IRS were integrated on the reactor to understand the chemistry happening inside. This was used to learn about how changes to process parameters influenced the fullerene formation and carbon evaporation. An iHR 550 spectrometer with a Syncerity 3000 CCD camera was used for OES. The OES was attached to a viewport by a fibre bundle cable on the reactor 10 cm above the plasma region. The detector was a synapse CCD detector. It was thermoelectrically cooled. An iHR 320 spectrometer with a Stanford Research Systems SR830 Lock-In Amplifier detector was used for IRS. An optical chopper was placed between the viewport on the reactor and the opening of the spectrometer. The detector was a solid-state liquid nitrogen-cooled detector made of indium, gallium and arsenide. The iHR 320 spectrometer sat on a metal plate and the center of the opening slit was set level to the center of the viewport. Finally, a LII-200 (laser induced incandescence) from Artium Technologies Inc. was used to monitor particle size of the carbon and fullerenes after they were treated by the plasma. LII-200 worked by using a laser pulse once every 20 nanoseconds to heat soot particles from ambient conditions to just below 4000 K [51]. The incandescence from the particles was detected by photodetectors. Complex analysis was done based on laser energy absorption by the soot particles and cooling time[51]. From this, volume fractions and particle sizes of the soot was calculated. The LII-200 used a venturi effect. A ¼-inch hose was connected to the reactor wherever a sample was needed to be taken from. Nitrogen gas at 25 SLPM was sent through the LII-200 sample chamber, which created a vacuum known as the venturi effect. This vacuum pulled a sample of soot from the reactor, sending it through the flow cell for analysis. The soot was then sent through a filter.

8.1.6 Collector

The collector's outer-shell was a stainless-steel (SS-304) chamber with a ceramic porous filter, and inside covered by a thermal filter sock. Carbon was exited at the top of the reactor and traveled through a 2-inch SS-314 tube and into the collector. The aerosol then hit the interior walls of the collector and fell into a hopper. The smaller particles deposited onto the filter. The exhaust helium exited the top of the collector and into the atmosphere. To collect the fullerene soot, the plasma was turned off. Argon gas was pulsed at 25 SLPM for 30 second intervals. This was done 5 times to push any remaining soot out of the reactor. After pulsing the reactor with argon, the gate valve to the collector was closed. The valve remained closed for at least 5 minutes to allow the carbon to settle. The bottom hopper was removed; the soot collected and the filter was brushed. A photo of the filter and thermal sock are shown in **Figure 14**.

Figure 14: Inside the collector, ceramic filter (black) and thermal filter sock (white). Attached to carbon steel flange and sealed using graphite gasket seals.

8.1.7 Reactor Body

Figure 15 is an AutoCAD drawing of the reactor used for the experiments. The image on the left displays the outer shell of the reactor. The 435.9 mm (outer diameter) carbon steel shell is the outer support for the reactor. Inside is a column of graphite crucibles. The graphite crucible in the plasma region is 89.4 mm (inner diameter) to account for the rapid expansion of the gases due to the steep temperature change. The internal diameter then decreases to 50.8 mm (inner diameter) for the remaining height of the reactor. In previous designs, the internal graphite crucible diameter gradually increased for expansion cooling to quench the fullerenes. This design was omitted, as it hindered the amount of carbon and fullerenes escaping the reactor and travelling to the collector. In the design shown below, a smooth transition from a larger to smaller diameter, maintained until the opening of the collector, allowed for a more controlled flow of the aerosolized product.

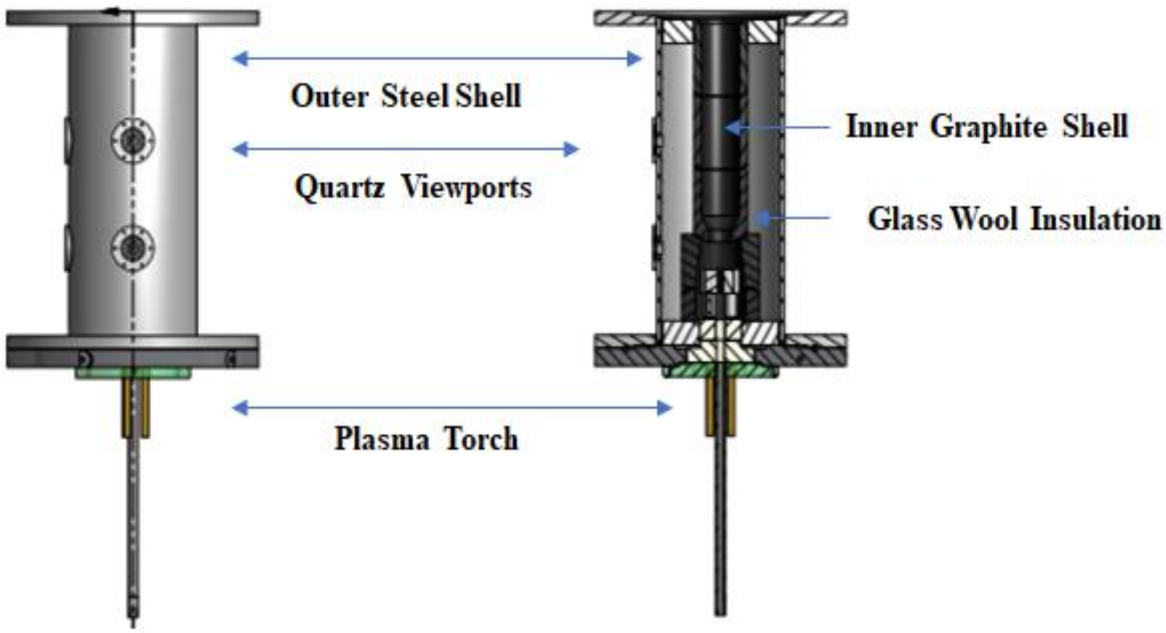

Figure 15: AutoCAD drawing of the 3-phase AC plasma reactor at the Applied Nanotechnology Lab. Left drawing shows the outer shell. Right drawing displays a cross-section of the reactor, displaying the internal structure.

8.1.8 Plasma Torch

The plasma torch is the heart of the reactor. Without it, the fullerenes could not be made. It is responsible for the energy to evaporate the carbon, which is the heat source that warms the entire reactor. The plasma torch for the 3-phase plasma reactor can be seen in **Figure 16**. The main housing for the torch is a G10 epoxy flange. G10 is a thermal and electrical insulator, essential for the design of the reactor. In a triangular formation, ¼ inch brass electrodes were fed through the G10 flange at its center. The tips of the brass were threaded and are connected to ½ inch graphite electrodes, which were machined to design. The graphite electrodes had internal threads that allowed for ¼-inch graphite nubs to screw in perpendicular to the brass. When in the correct orientation, the nubs were oriented 120^{o} and had a gap of approximately 1 mm.

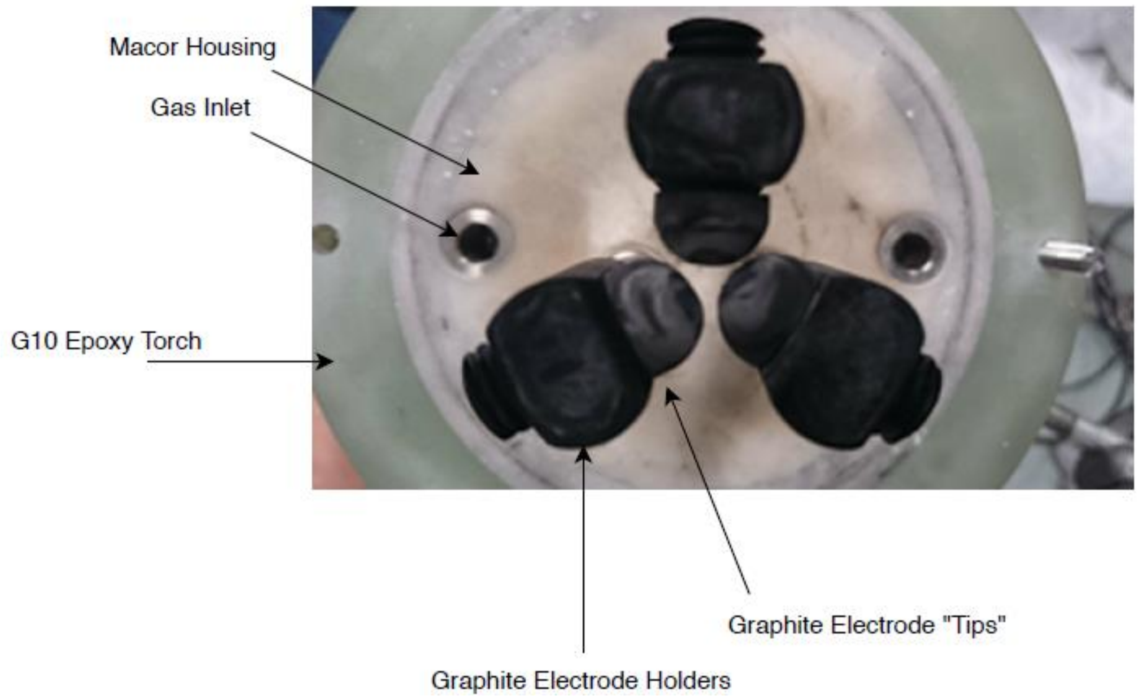

Figure 16: Top view of the plasma torch for the fullerene reactor.

The brass electrodes were hollow until the threaded tips. A 1/8-inch SS-314 tube was sent through the hollow center of the brass. This allowed for internal water cooling. Water was sent through the small stainless-steel tube, and flowed around the annulus of the yellow brass, exiting back into the chiller to finish the loop. On the exterior of the brass, wire connectors were attached. These connected to each of the three wires coming from the power supply.

On top of the G10 and inside the reactor, there was an alumina disk. The purpose of the disk was to act as a heat shield for the G10. Radiation and convection from the plasma caused the G10 to melt, since it has a low melting temperature of 135^{o}C. However, the use of the alumina heat shield as a thermal insulator prevented this from happening.

8.2 Fullerene Reactor Experimental Procedure

There are some important steps that must be followed in the formation of fullerenes. These steps are essential to both the formation of fullerenes and the safety of the operators. These include plasma ignition, reactor pre-heating, carbon feed/experimental run, reactor cool down and collection.

8.2.1 Plasma Ignition

It was a two-person job to ignite the plasma. One person controlled the power switch while the other handled the ignitor. The following steps were followed:

1. The plasma torch was screwed into the bottom flange using six 1/8-inch threaded rod and nuts holding it in place.
2. Gas flow was set to 10 SLPM at the torch, 3 SLPM at the viewports and 3 SLPM at the top and flowing for at least a minute in argon.
3. The ignitor was placed (a rod with graphite at the tip) in contact with all three graphite electrodes.
4. The power source was turned on and the ignitor was kept in contact with the graphite electrodes until the plasma ignited.
5. The ignitor was taken away and the plasma was left to stabilize for at least a minute.
6. The gas flow rate was set as desired.

8.2.2 Reactor Pre-Heating

Pre-heating the reactor was an essential step taken in order to have control over the annealing process of the fullerenes. If the reactor was room temperature in the zones directly after the plasma zone, the product would contain mostly carbon black and negligible amounts of fullerenes. This controlled cooling, or annealing, was crucial for fullerene formation. Therefore, it was necessary to have the entire reactor at least 550^{o}C, which is well above the sublimation temperature of fullerenes. The following steps were taken to pre-heat the reactor:

1. The plasma was ignited in argon gas and the gas flow rate was increased to 25 SLPM at the plasma region.
2. The plasma was kept running until the reactor temperature reached 550^{o}C. This was monitored using N-type thermocouples and LabView software.
3. OES and IRS were turned on to begin spectroscopic data collection.
4. If the temperature of the power supply exceeded the operating temperature, the pre-heat was stopped. The gas flow rate was lowered to 3 SLPM at the torch until the power supply cooled to at least 40^{o}C. Steps 1 to 3 were repeated until the minimum internal reactor temperature was 550^{o}C.

8.2.3 Experimental Procedure for Feed Runs

The experimental procedure was the most important step to produce fullerenes:

1. The Tekna powder feeder was set to the experimental mass flow rate of carbon feedstock by adjusting the central motor/impeller speed.

2. The plasma gas was changed from argon to helium. The gas flow rate was set to the experimental flow rate (10 – 18 SLPM). The reactor was purged with helium for at least 10 minutes to remove any residual argon.
3. The plasma was ignited as per the procedure in section 8.2.1 and left to stabilize for at least 1 minute before feeding carbon.
4. Spectroscopic data collection started once the carbon feeder was turned on.
5. Carbon was fed for at least 5 minutes, or until the power supply reached its operating limit.
6. After 5 minutes of feeding carbon, the powder feeder was turned off, but the plasma remained on. This allowed for any residual carbon in the reactor falling toward the plasma to evaporate again.
7. The plasma was turned off after 1 minute. The gas was changed to argon, so helium was not wasted. The gas flow rate at the torch was set to 25 SLPM.
8. The reactor was cooled to at least 400^{o}C.
9. At 400^{o}C, pulses of argon gas were sent through the plasma torch to push any remaining carbon towards the collector.
10. The soot was collected and weighed in a clean and dry plastic container. The container was wrapped with foil to limit light exposure.

It is important to state here that since the inductors used on this reactor were modified transformer, they did tend to heat up over time. It was necessary to have one operator use a thermal camera to monitor the inductor an transformer temperature at all times during the experiment. The operational limit of the transformer and inductors was 240^oC. Since the thermal camera only monitored the surface temperature, the experiment was ceased at 40^oC below the operational limit. This was to ensure no thermal degradation of the power supply.

8.3 Offline Sublimator Set-up

The offline sublimator, illustrated in **Figure 17,** was used for the preliminary tests of fullerene IR emission at UNB. Shown below is a 3-zone tube furnace, and inside is a 1-inch quartz tube. Placed inside this tube, is a ceramic boat filled with either C_{60}, C_{70} or fullerite. At each end of this tube is an aluminum flange. These flanges allowed for gas and vacuum connections, and they sealed the tube. On the right-most flange is a viewport, which is a KBr disc. KBr was used because it transmits IR, whereas quartz does not. The tube furnace had internal temperature controls at each of the 3 zones. Finally, an iHR 320 purchased from HORIBA Scientific was placed at the end of the viewport for analysis. Following the lines, light and IR entered the spectrometer and was reflected on a series of mirrors and gratings, until exiting the spectrometer into the detector. The detector is single-channeled and liquid nitrogen cooled. Incident light triggers a response on the detector, which caused a voltage change, and this information was then sent to a lock-in amplifier to amplify the voltage. Then, the Lock-in amplifier sends this information to the computer, and the corresponding voltages versus peak position in nanometers were plotted.

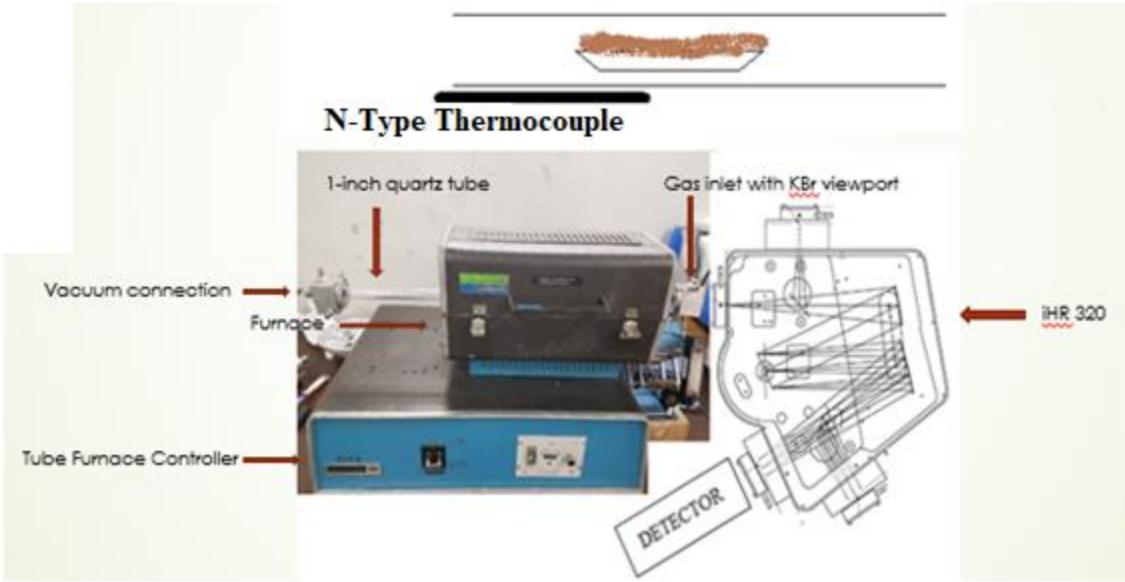

Figure 17: Offline sublimator set-up at the Applied Nanotechnology Lab at UNB[52].

8.3.1 Offline Sublimator Experiments

An offline sublimator was used as a proof-of-concept experiment. A tube furnace with a 1-inch quartz tube was used. Aluminum flanges were designed and placed at each end of the quartz tube. This allowed for gas flow, a vacuum pump hook-up, a thermocouple attachment and a sealed tube. Inside, a ceramic boat filled with either C_{60}, C_{70} or fullerite was tested. The tube furnace controlled the temperature of the system by using a potentiostat and a N-type thermocouple. These experiments were done to test if there was a trend in peak intensity versus tube furnace temperature. Based on **Figure 18**, as temperature increases, the vapour pressure of fullerenes also increases. As known from the ideal gas law (**Equation 1)**, as pressure increases, moles increase. Therefore, by increasing the temperature of the tube furnace, the number of fullerene molecules in the gas phase that are emitting IR should also increase. In turn, this increased emission should correlate to a higher peak intensity/area.

$$PV = nRT$$

Equation 1: Ideal gas equation. P represents pressure of the gas, V is the volume occupied by the gas, n is the moles of gas in the system, R is the ideal gas constant and T is the temperature of the gas.

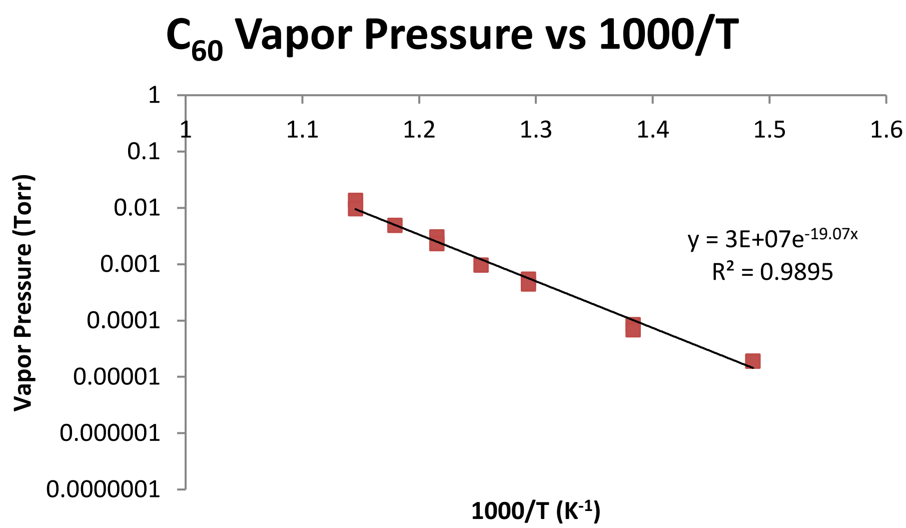

Figure 18: Fullerene vapour pressure as a function of temperature[53].

8.3 Off-line Sublimator Experimental Procedure

The off-line sublimator experiments were used to generate a calibration curve. The calibration curve was used to compare the IR emission data obtained from the experiments done on the reactor. From this, fullerene concentration inside the reactor was determined theoretically. The following steps were taken for the off-line sublimator experiments:

1. Fullerite, C_{60} or, C_{70} was weighed and transferred to a clean and dry ceramic boat.
2. The boat was placed in the center of the 1-inch quartz glass tube using a quartz rod.

3. The aluminum flanges were sealed onto each of the quartz tube ends by compressing an o-ring.
4. The tube furnace was heated to 150^{o}C, once everything had been tightened.
5. The diaphragm vacuum pump was turned on to remove any atmospheric gases and moisture adsorbed to the fullerenes. A continuous slow flow of argon was maintained to provide a positive pressure inside the gas feed lines.
6. The temperature was maintained at 150^{o}C for at least 5 minutes.
7. The temperature increased to the experimental temperature (300^{o}C-800^{o}C) with the vacuum on and argon flowing.
8. Once the desired temperature was reached, argon was turned off and allowed the vacuum to pump the quartz tube to -30 psi (gauge pressure). This was done for 2 minutes. Then the ball valve was closed, and the pump shut off.
9. IRS data collection was completed.

8.4 On-line Diagnostics Operational Procedure

Research and preliminary experiments were done to determine what setting was to be used for the online diagnostics. The OES and IRS operations are quite similar since they are purchased from the same company, HORIBA. The spectrometers are almost identical (just different models), however, the operation of the LII is quite different.

8.4.1 General Procedure for the Optical Emission Spectrometer

1. The iHR 550, shutter control box and CCD camera were turned on. The LED light changed from orange to green. This indicated that the thermoelectric cooler had cooled the detector to -40^{o}C.
2. The spectrometer entrance slit was set to 2 mm and the exit slit to 2 mm. The integration time was set to 0.01 seconds.
3. The 2400 grooves/mm grating was used because precise measurements were needed.
4. To calibrate the iHR 550, a light source with a known monochromatic wavelength was used. It was a green laser with a monochromatic wavelength of 532 nm.
5. The laser was place at the end of the fibre optic cable and into the spectrometer.
6. Using the “Real Time Control” function in the SynerJY V 3.5 software, the peak from this light source was given.
7. The wavelength range was changed until the peak was in the middle of the spectrum with a minimum intensity of 60000 arbitrary units. The iHR was then calibrated.
8. The above calibration process was done for the other two gratings.
9. SynerJY V3.5 software provided by HORIBA Scientific was used to analyze the OES. A “Batch Experiment” was created by selecting a wavelength range that covers the Swan Bands, and 300 nm-600 nm was used.
10. The experiment was saved in a folder and exported to another software for analysis with Origin Pro. This software allowed for the analysis of peak position and peak area.

8.4.2 General Procedure for the Infrared Radiation Spectrometer

1. The Lock-in amplifier was turned on and was warmed up for at least an hour.
2. Ten-minutes before beginning the experiment, the liquid nitrogen dewer surrounding the detector (InGaAs solid-state detector) was filled.
3. The same software provided by HORIBA Scientific was used and the spectrometer entrance slit was set to 2 mm and the exit slit to 2 mm.
4. The calibration was done the exact same as it was for the iHR 550, however instead of having gratings 600, 1200 and 2400 grooves/mm, the iHR 320 had 150, 300, and 1200 grooves/mm.
5. Again, in SynerJY V3.5, a "Batch Experiment" was created covering the peaks given by C_{60}. The wavelength ranges chosen were 6900 nm-7100 nm, 8400 nm-8600 nm and 17300 nm-17500 nm for the 7000 nm, 8500 nm and 17400 nm peaks, respectively.
6. A scan typically took about 5 minutes, so only one cycle was needed for each reactor experiment. For the off-line sublimator experiments, at least 3 scans were completed for each peak.
7. In addition, only the 17400 nm peak was chosen for the reactor experiments because it was stated in the literature that the 7000 nm peak and 8500 nm peak overlap with PAH peaks.
8. The spectra were saved and exported to Origin Pro software and analysis was done like the OES.

8.4.3 General Procedure for the Laser Induced Incandescence

1. The LII chiller, computer, control box and the laser manifold were turned on, in that order.
2. The sample cell temperature was set to 200^{o}C to ensure minimal moisture.
3. AIMS software provided by Artium was used.
4. Nitrogen gas flow was turned on and the valve on the sample cell was opened to create the venturi effect.
5. The valve connected to the reactor, where the sample was taken from, was opened.
6. After the data was collected, everything was shut down except the chiller. This allowed the sample cell to cool to room temperature.

8.5 Soot Analysis

The soot collected from the 3-phase plasma reactor was stored in a plastic container wrapped in aluminum foil. From here, the sample was brought to Enterprise Building 2 for analysis. To determine the yield, the soot was dissolved in 1,2,4-trimethylbenzene (TMB) and ran through a HPLC. A COSMOSIL 5PBB Packed column inside the HPLC was used to separate the fullerenes dissolved in the TMB. Lighter fullerenes eluted faster than heavier fullerenes. The HPLC was equipped with a photodiode array detector that could detect absorbed wavelengths in the UV-Vis spectrum, with a low signal-to-noise ratio. The effluent was sent through the detector where a spectrum for each corresponding fullerene was displayed according to its retention time. Calibrations were done to measure the retention time (**Table 6**) for each fullerene and each corresponding UV-Vis spectrum. A calibration curve was constructed to determine concentration of C_{60} and C_{70} in TMB, measured in mg/ml.

Shown in **Figure 19 is** a Hewlett Packard (Agilent) 1090 series II HPLC used to analyze fullerene soot quantitatively and qualitatively. **Table 4** and **table 5** outline the HPLC sample preparation and operating parameters, respectively.

Figure 19: HP 1090 Series II HPLC.

Table 4: Parameters for HPLC sample preparation.

SAMPLE PREPARATION	
Sample Concentration	20 mg soot/ 5 grams TMB
Sonication Time	30 Minutes
Centrifuge Setting	Room Temperature, 2400 RPM
Centrifuge Time	20 Minutes
Sample Transferred to HPLC Vial	3 mL of supernatant

Table 5: HPLC operation parameters for fullerene analysis.

HPLC OPERATION PARAMETERS	
Mobile Phase	1,2,4-trimethylbenzene
Mobile Phase Flow Rate	1.000 mL / min
Pressure	130 bar
Sample Injection Volume	25.0 µL
Experiment Run Time	10 minutes
Column Temperature	24^{o}C

The effluent was collected in a waste container labelled "TMB+Fullerene waste" and sent for TMB recycling. The peak analysis was done using a peak analyzer provided by the software, and manual modifications to the area were done if necessary. A Microsoft Excel spreadsheet with the previously made calibration curve was prepared, and new peak areas were entered in the spreadsheet to determine the area and yield of the collected fullerenes.

Table 6: Fullerenes retention time in the HPLC using the COSMOSIL 5PBB Packed column.

Fullerene	Retention Time (min)
C_{60}	4.3
C_{70}	5.3
C_{76}	6.1
C_{78}	6.4
C_{84}	7.3

Figure 20 represents a typical chromatograph of the soot samples collected from the reactor. As shown on the graph, C_{60} has the highest peak intensity, and C_{70} is roughly half of C_{60}. This is the typical relative abundance of C_{60} and C_{70} found in most fullerene soot. From the chromatograph, peak area determines the concentration of each species. The greater the peak area, the higher the concentration.

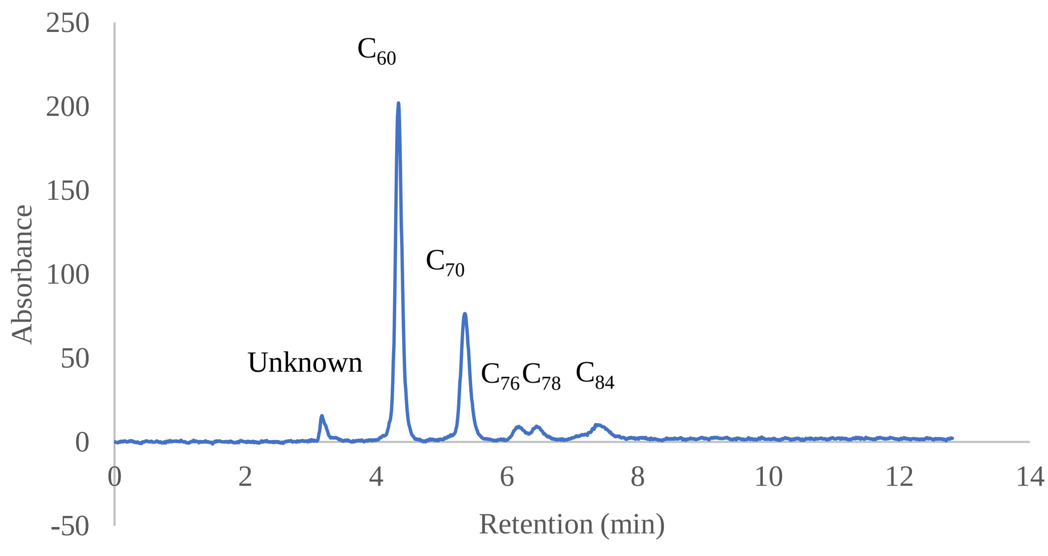

Figure 20: A sample high-performance liquid chromatograph of a soot sample collected from the 3-phase AC plasma reactor.

8.6 Assumptions

For the purposes of this research, the following assumptions were made:

1. Products and reactants did not interact with each other or the internal structure of the reactor, as carbon is a relatively inert element.
2. Since the gases were operated at a relatively low pressure (400kPa), it was assumed they would not deviate from ideality. Therefore, all gases were assumed to be ideal.
3. The amount of carbon collected in the soot due to thermal erosion of the graphite electrodes was negligible compared to the amount of carbon fed in as an aerosol.
4. Due to design limitations of the reactor, approximately 30% of carbon fed was collected as soot. It was assumed that the yield of the collected soot was representative of the yield as if there was 100% collection.
5. It was assumed that fullerenes do not react with the material of the filter sock, the inner graphite walls or the steel tubes.
6. The infrared signals given at 17.4 µm was due to C_{60} alone.
7. It was assumed that any CN peaks in the OES were due to atmospheric air entering the reactor during maintenance.
8. All fullerenes in the soot sample dissolved in the 1,2,4-trimethyl benzene solvent and no unreacted carbon dissolved.
9. HPLC peak response to C_{76}, C_{78} and C_{84} were equivalent to C_{70}.
10. Emission from fullerenes was in all directions and of equal magnitude.

8.7 Scope and Limitations

The main purpose of this investigation was to determine whether fullerenes could be detected on a reactor using IRS. Due to limitations of the spectrometer, a sweeping scan was not done. Instead, a narrow range from 17.3 µm-17.5 µm was chosen. The iHR 320 did not have a sweeping scan setting, but instead focused on one wavelength at a time.

Since the operation limit for G10 is 130^{o}C, a ceramic heat shield (a fire brick purchased from KENT) was used to protect it. To ensure there was no overheating, it was determined that a minimum gas flow of 10 SLPM was needed to push the plasma upward. This alleviated any disintegration of internal reactor parts.

Even though the power source was specified for 45 kW of power, the power supply would still overheat during operation. Depending on the current of the plasma, the pre-heat and experiment time solely depended on the rate of overheating from the power source. Due to this, continuous operation was not feasible. After the plasma was extinguished, the power source required at least 15-minutes to cool down before it could be used again.

Since it was required to remove the plasma torch after each experiment, it was impossible to stop the diffusion of ambient air into the reactor. Therefore, atmospheric gas could absorb onto the interior surface of the reactor.

IRS and OES experiments were done merely as a proof of concept. This is because there was too much interference (noise) inside the reactor to truly state whether there was a direct correlation between signal intensity and carbon/fullerene concentration in the gas phase.

The laser induced incandescence samples were not taken from the reactor, as this would have affected yield and collection efficiency. This device was used to test if any carbon was escaping after the filter, to determine if the collection method was enough.

Based on the error of the grating chosen for IRS, it was assumed that any peaks shown in the range 17350-17450 nm were to be C_{60}. Since the spectrometer could not perform sweeping scans, if multiple peaks were present, they were all assumed to be C_{60}.

During the offline sublimator experiments, it was impossible to put a thermocouple inside the quartz tube, as it would have severely affected the results of the experiment. The n-type thermocouple was placed on the outside of the tube furnace touching the wall. Since the temperature was held constant for approximately 15 minutes, it was assumed that contents inside the tube, including gases and solids, reached the same temperature as the outer glass wall.

9.0 Results and Discussion

The results of the optical emission spectrometer, offline sublimator experiments, reactor experiments and yield analysis will be presented in this section. Results from the offline sublimator experiments were used as a calibration of fullerene concentration in inert gas.

9.1 Optical Emission Spectroscopy Results

As stated previously, carbon black evaporates at 4287^{o}C[24]. The energy produced from either argon or helium plasma contains sufficient energy to evaporate carbon black[47]. Therefore, feeding aerosolized carbon black through an argon or helium plasma should evaporate the carbon black. Once the carbon has been evaporated, it immediately forms carbon dimers, and subsequently emits visible green light. If more carbon evaporates (i.e. a higher efficiency in the rate of vaporization of carbon black), a more intense emission of visible green light would be observed. As stated in section 8.2.2, two pre-heats were necessary to ensure that the entire reactor was at a suitable temperature for fullerene production. The temperature read by the N-type thermocouples can reach 900^{o}C. At these elevated temperatures, an increased efficiency of the vaporization of carbon is expected.

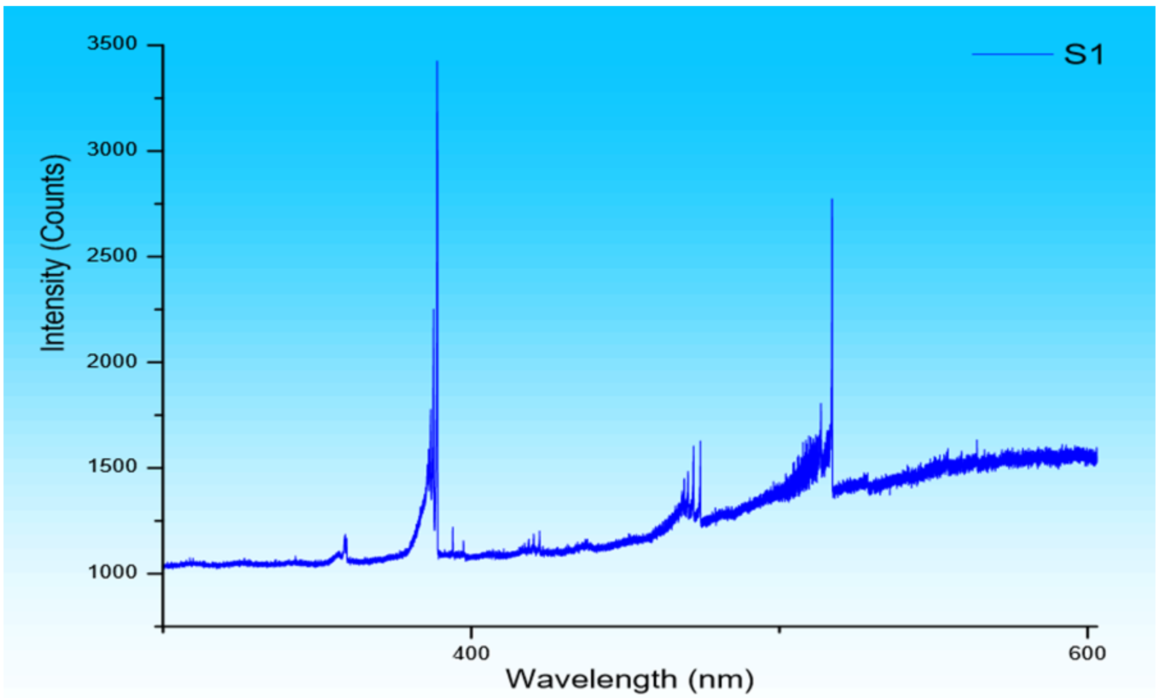

Figure 21: Optical emission spectrum of the AC plasma reactor during the first pre-heat stage in argon plasma.

Measurements derived from **Figure 21** are summarized in the table below:

Table 7: Peak position, intensity and peak characterization of an OES in argon plasma preheat stage 1.

Peak Position (nm)	Intensity (arbitrary units)	Characterization
389	3426	CN
474	1628	C_2
517	2774	C_2

Table 7 indicates the major peaks seen in **Figure 21**. However, there are still peaks present at 360 nm, 425 nm and 550 nm, which represent CN, C_2 and C_2, respectively. Upon comparison of the relative intensities of the major peaks presented above, CN is the most abundant. This is because there is a nitrogen impurity present in the 99.95% argon plasma gas. At these temperatures the reaction between nitrogen and carbon are more favourable than carbon-carbon reactions.

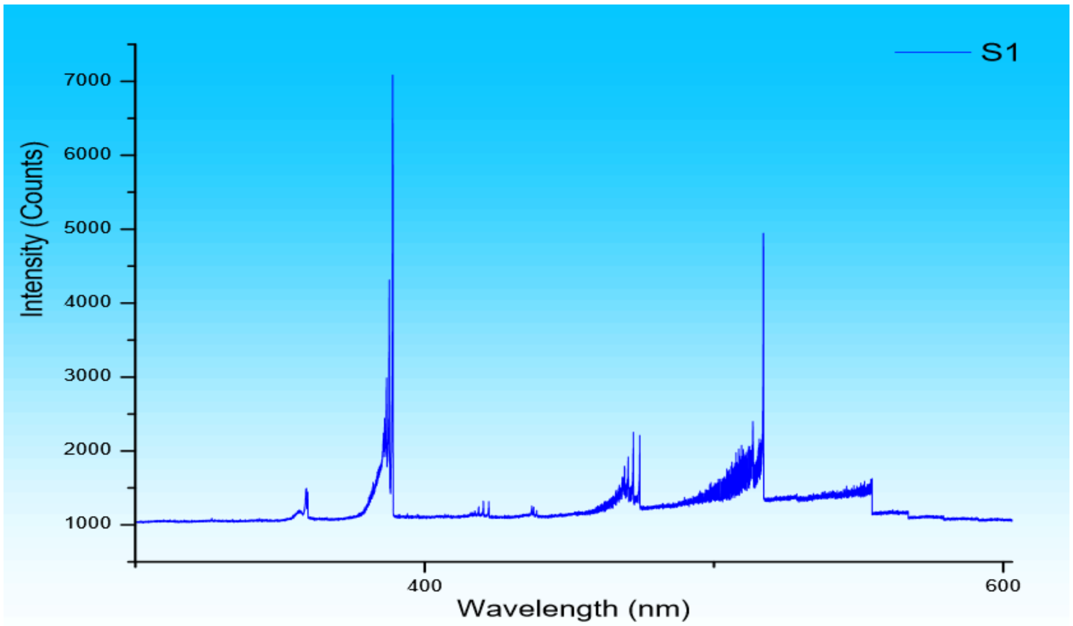

Figure 22: Optical emission spectrum of the AC plasma reactor during the second pre-heat stage in argon plasma.

Measurements typical of **Figure 22** are summarized below:

Table 8: Peak position, intensity and peak characterization of an OES in argon plasma preheat stage 2.

Peak Position (nm)	Intensity (arbitrary units)	Characterization
389	7086	CN
474	2274	C_2
517	4946	C_2

It was hypothesized that as the internal temperature of the reactor increased, there would be a greater vaporization rate of carbon. Based on the increased intensities of the peaks present in **Figure 22**, this theory is validated. However, it was seen that there was a greater peak intensity from CN species than C_2 particles. This is due to argon plasma not being as hot as a helium plasma. There is more than enough energy to dissociate nitrogen gas to its reactive elemental form. However, there is just enough energy present to evaporate the solid carbon feedstock.

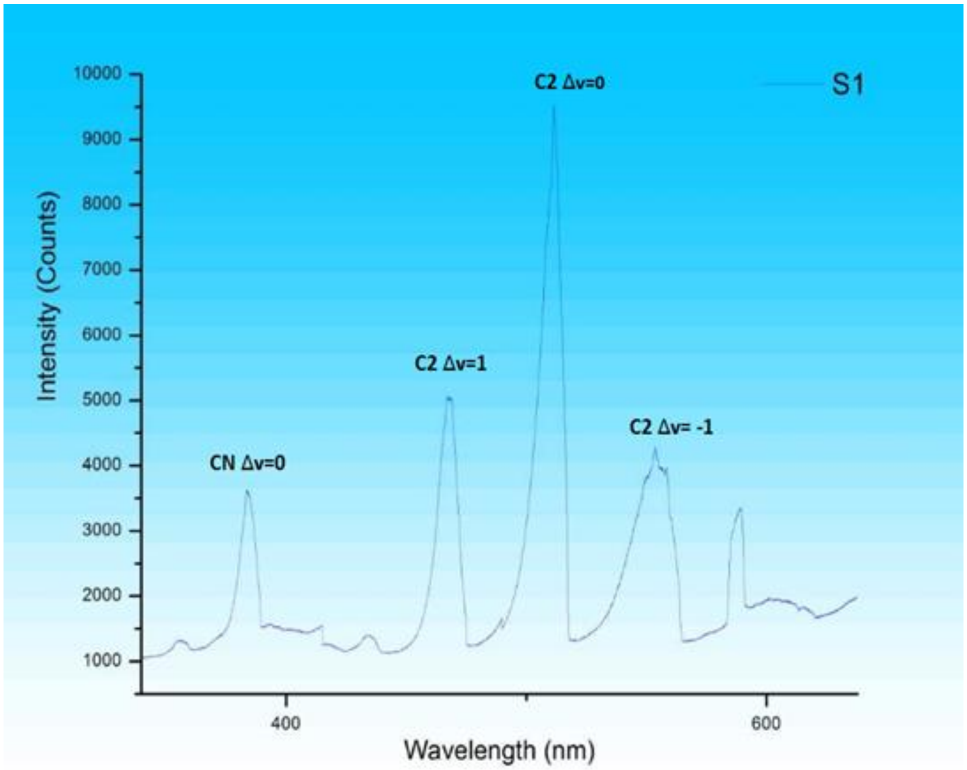

Figure 23: Optical emission spectrum of the AC plasma reactor during carbon feed in helium plasma.

Measurements derived from **Figure 23** are summarized below:

Table 9: Peak position, intensity and characterization of an OES in helium plasma with carbon feed.

Peak Position (nm)	Peak Intensity (arbitrary units)	Characterization
390	3500	CN
475	5000	C_2
510	9750	C_2
550	4700	C_2

Due to the increased thermal conductivity of helium, a hotter plasma is generated. This hotter plasma will evaporate more carbon than an argon plasma does. The helium used for these experiments was the same percent purity as the argon, at 99.995%. Therefore, the relative concentration of nitrogen to plasma gas should be the same. Comparing the spectra above, it is indicative that there is a drastic change in the I_{C2}/I_{CN} ratios.

Table 10: Comparing the I_{C2}:I_{CN} ratios for the three different optical emission spectra above.

Plasma Gas	I_{510}/I_{390}
Ar (Preheat 1)	0.81
Ar (Preheat 2)	0.70
He	2.79

As shown in **Table 10**, helium plasma has a much higher concentration of carbon dimers than CN radicals. The higher thermal conductivity leads to an increase in the energy available. This allows evaporated carbon to react with other carbon species more favorably compared to nitrogen radicals. The opposite is seen in an argon plasma. Since there is a lower thermal conductivity, a colder plasma causes carbon to react more favorably with nitrogen radicals. It was seen that there was a significant change in the ratio of C_2/CN in argon plasmas. This indicates that argon plasma does not sufficiently evaporate carbon.

The spectra given from the OES provides a lot of information regarding the chemistry happening in the reactor. The information provided allows chemical engineers to have the opportunity to optimize the reactor. Relative concentrations of C_2 with respect to CN for various conditions can be determined. In addition, using the same peak broadening theories as discussed above, the velocity of the gaseous C_2 can be determined. By knowing the velocity and the cross-sectional area of the reactor, the residence time of C_2 can be determined. As chemical engineers, residence time of any reaction is a crucial parameter to determine sizing of reactors.

$$\frac{\Delta\lambda}{\lambda} = \frac{v}{c} = \left(\frac{1}{c}\right)\left(\frac{\sqrt{2kT}}{m}\right)$$

Equation 2: Thermal line broadening of a spectral line. $\Delta\lambda$ is the peak width at half max (nm), λ is the peak position (nm), c is the speed of light (299,792,458 m/s), v is the velocity of the emitting species (m/s), k is the Boltzmann constant (1.3807×10^{-23} J/K), T is the temperature of the emitting species (K), and m is the mass of the emitting species (kg).

Based on the thermal line broadening of a spectral line described in **Equation 2**[54], both the velocity and temperature of the gaseous species can be determined.

Table 11: Velocity, volumetric flow rate and residence time of C2 dimers in the reaction zone of the 3-phase plasma reactor. Peak of interest is at 510 nm. Argon 1 refers to pre-heat 1, Argon 2 refers to pre-heat 2, and Helium refers to plasma run with helium gas

Experiment	**$\Delta\lambda$ (nm)**	**Temperature (K)**	**Area (m^2)**	**Vol. Flow Rate (m^3/s)**	**Volume (m^3)**	**Res. Time (s)**
Argon 1	0.1	5000	7.79E^{-3}	457.8	1.56E^{-5}	3.40E^{-8}
Argon 2	0.4	Unreliable	7.79E^{-3}	Unreliable	1.56E^{-5}	Unreliable
Helium	10	Unreliable	7.79E^{-3}	Unreliable	1.56E^{-5}	Unreliable

From the results shown in **Table 11**, in hotter plasma, the C_2 particles have higher kinetic energy than they do in colder plasma. This results in C_2 having a higher velocity as it passes through the reaction zone of the reactor. This increased temperature ultimately influences the residence time. It is known that residence time is a very important design parameter. The fact that spectroscopy can be used to find the residence time of C_2 (fullerene building blocks) enables engineers to use fundamental design equations to both optimize and scale a reactor of this type accordingly. The argon 2 and helium experiments provided unreliable information. Since the peak widths were so large, the temperatures and residence times calculated were astronomically high. At these conditions inside the reactor, the rotational and vibrational transitions begin to overlap with the electronic emission peak. There were unresolved vibrionic transitions contributing to the overall peak width. This contributes to an inaccurately large peak width. Ultimately, a spectrometer with a higher resolution would be able to detect each of these transitions so accurate peak widths can be obtained. The seemingly low residence time of 3.40×10^{-8} seconds does seem alarming, but when comparing to how to how long it takes to form fullerenes (picoseconds), this value makes sense[45]. Finally, the temperature of 5000 K is in accordance with literature values of C_2 formed in argon plasmas[47]. With this information, the use of spectroscopy as a diagnostic tool for fullerene production is very advantageous if there are no unresolved vibrionic transition contributing to the overall peak width.

9.2 Off-line Sublimator Experimental Results

The off-line sublimator experiments were done via the procedure outlined in Section 8.4.2. The temperatures tested were 300°C-800°C in 100°C intervals. Only data from 7.0 µm, 8.5 µm and 17.4 µm were taken. The IR active peak for C_{60} at 18.9 µm was omitted. This was because from trial-and-error experimentation, at temperatures above 400°C, the signal from this IR active mode saturated the spectrometer. Because of this, the spectra recorded at these temperatures were inconclusive.

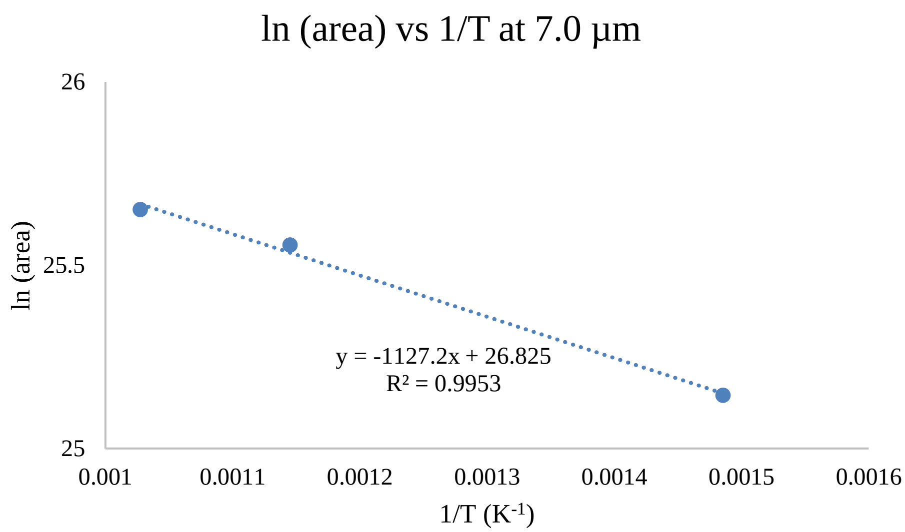

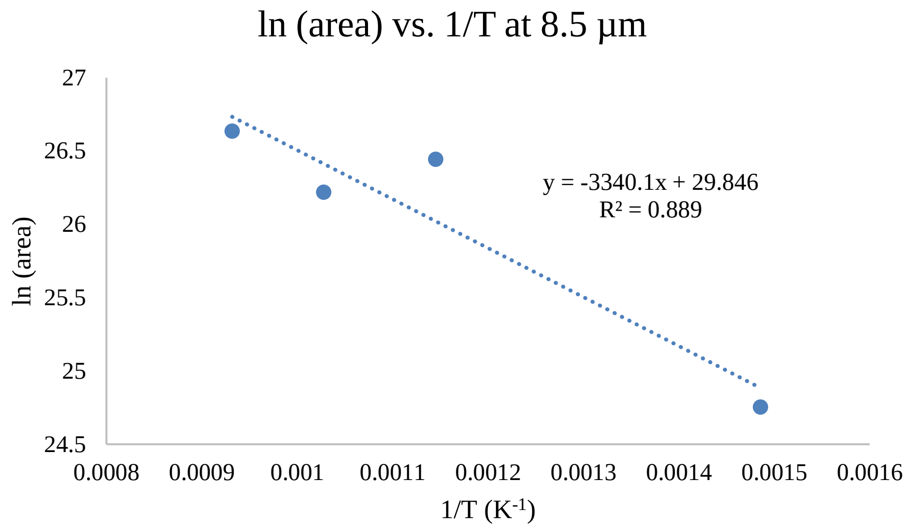

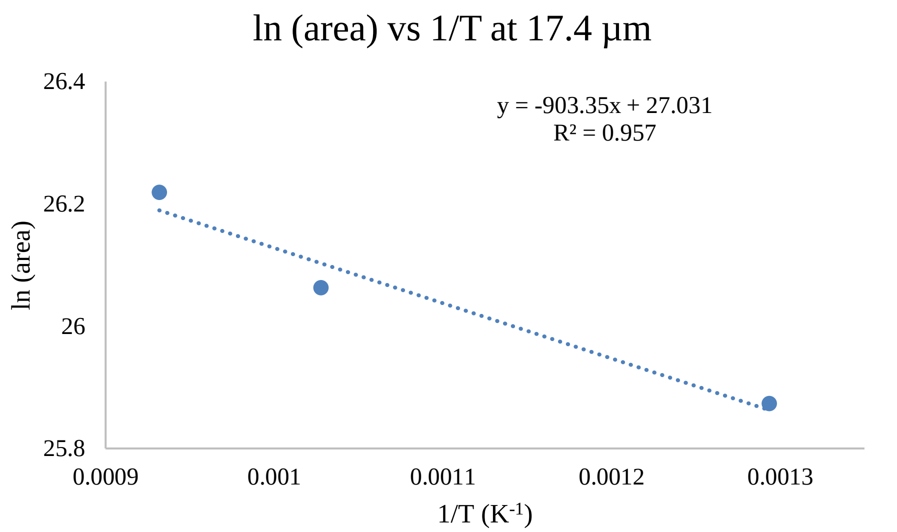

Figure 24: Results obtained from the offline sublimator experiments. ln(area) vs 1/T have been plotted for data points taken at 7.0 µm, 8.5 µm and 17.4 µm respectively.

From the data shown in **Figure 24**, the natural logarithm of the peak area was plotted versus inverse temperature as anticipated in the Clapeyron relation. It was found that as temperature increased, the area under-the-curve for the IR signal also increased. Based on the results from researchers in **Figure 25**[55], there is a linear relationship between the logarithm of fullerene vapour pressure and temperature. Relating the vapour pressure to the number of moles of fullerenes using the Ideal Gas Law, the relative concentration of fullerenes in the gas phase can be determined. Using the IRS, the area under-the-curve represents the signal strength. The signal strength increases as more molecules are emitting IR, representing a higher vapour pressure.

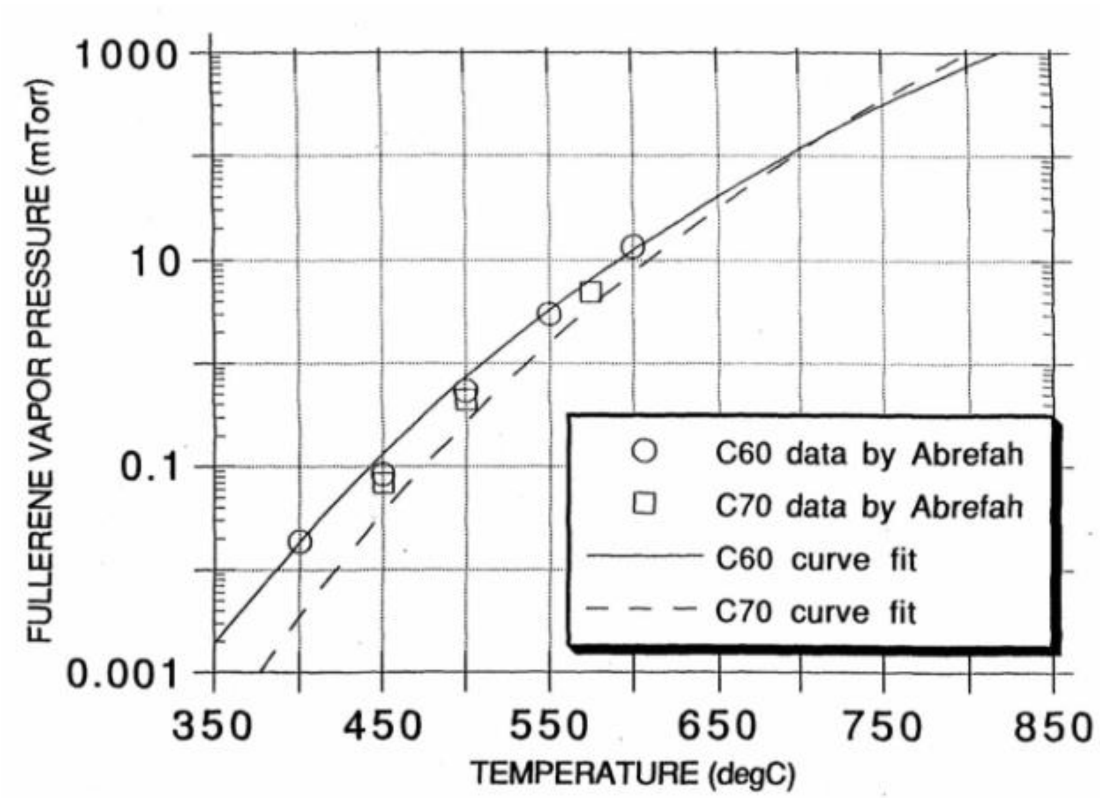

Figure 25: Vapour pressure of fullerenes as a function of temperature[55].

From this newly gained information, the trend from the off-line sublimator experiments indicated that there was an increase in the number of fullerenes in the gas phase as temperature increased. For the purposes of this proof-of-concept research, only repeated temperatures with consistent results were considered. Data points at temperature intervals that gave IR areas spanning a wide range (i.e. high standard deviation), were not considered. For this reason, there are only three data points in the above graphs. **Table 12** shows the data collected from the experiments in the IR active mode at 7.0 µm. An increase in temperature from 673 K to 873 K caused an area increase of 50%. An increase in temperature from 873 K to 973 K caused a 10% increase in the area of the IR active signal. As temperature increased, the rate of change of vapour pressure decreased. This trend is shown in **Figure 25**. This means that the slope of the tangent line to the curve decreases. It would be expected that at higher temperatures, an increase in temperature would have a lesser effect on the vapour pressure, compared to the same change if the initial temperature was lower. Based on the results in **Table 12**, it was shown that the area under-the-curve follows a similar trend.

Table 12: Data obtained from IRS experiments for 7.0 µm. Temperature, 1/T, area under-the-curve and the natural logarithm of the area were recorded.

Temperature (K)	**1/Temperature (K^{-1})**	**Area**	**Ln(Area)**
673.15	0.00149	8.32E+10	25.145
873.15	0.00115	1.25E+11	25.554
973.15	0.00103	1.38E+11	25.651

Table 13: Data obtained from IRS experiments for 8.5 μm. Temperature, 1/T, area under-the-curve and the natural logarithm of the area were recorded.

Temperature (K)	1/Temperature (K^{-1})	Area	Ln(Area)
673.15	0.00149	5.63E+10	24.754
873.15	0.00115	3.05E+11	26.444
1073.15	0.0000932	3.69E+11	26.635

.

Table 14: Data obtained from IRS experiments for 17.4 μm. Temperature, 1/T, area under-the-curve and the natural logarithm of the area were recorded.

Temperature (K)	1/Temperature (K^{-1})	Area	Ln(Area)
773.15	0.00129	1.72E+11	25.873
973.15	0.00103	2.08E+11	26.063
1073.15	0.00932	2.44E+11	26.219

The same experiments were performed for the IR active modes at 8.5 μm and 17.4 μm. The results from 8.5 μm IR active mode experiments were very sporadic. However, the opposite was observed for the 17.4 μm IR active mode. The increase from 773 K to 973 K caused a 20% increase in area, and the increase from 973 K to 1073 K caused a 17% increase in area. This is quite interesting, as it does not follow the same trend outlined above. At higher temperatures, it was shown that there was a greater number of molecules emitting with changes in temperature. Because of this trend, and the fact that 17.4 μm gives the strongest signal, the IR active mode at 17. 4 μm was chosen to be studied on the reactor as well.

9.2 Infrared Emission of Fullerenes on a 3-Phase AC Plasma Reactor

With the success of the IR emission experiments on the off-line sublimator, similar experiments were performed to determine the effect of fullerene emission on an operating 3-phase plasma reactor. The intent of these experiments was to see if fullerene signal could be detected on an operating reactor. If so, could there be a relationship between fullerene signal and concentration of carbon fed? The second condition would be extremely challenging. This is because there are multiple parameters to consider. The plasma is a large blackbody emitter, and unreacted carbon black is a very good infrared absorber. The surrounding graphite walls would reach temperatures greater than 600^{o}C, which would also emit IR. With all this interference, it would be very difficult to observe any trend in IR emission and carbon concentration. Nonetheless, this investigation was a proof-of-concept experiment.

After rigorous experimentation on the reactor in conjunction with another project, three gas flow rates at three different carbon feed rates were tested. A compilation of the yield results is contained in Anshuman Sarawagi's PhD dissertation (2019). For the purposes of this thesis, the maximum yield of collected fullerenes was 13.83%. This result is ground breaking as the highest recorded yield at atmospheric pressure operation. The IR emission signals observed from this experiment and an experiment where the collected fullerene yield was 5.40%, were roughly equal. Based on the off-line sublimator experiments, a similar signal strength would indicate similar amounts of gaseous fullerenes. On the contrary, for the results gathered from the experiments performed on the reactor, the trend does not match. The overall yield is less than half, yet the signal strengths are very similar.

10.0 Conclusion

The purpose of this research project was to see if the use of spectroscopy was a useful real-time detector of fullerenes and for monitoring the conversion of carbon feedstock to C_2 vapour. The types of spectroscopy explored were OES and IRS. To determine if there was a relationship between the emission spectra and temperature of the emitted fullerene, an off-line sublimator experiment was developed. It was found that as temperature increased, the emission strength of fullerenes increased as well. The emission intensity, and area under the curve of the corresponding peak increased as temperature increased. These results matched the hypothesis. The increased emission strength was related to the number of fullerene molecules emitting IR in the gas phase.

After these results were obtained, the viability of real-time spectroscopy on an operating reactor was tested. The results from these experiments were not as promising. The emission strength from fullerenes were inconsistent. Yields that differed by factors of two and three had the same emission strength. The only explanation for these results could be that there is too much interference impeding the emitted IR signal reaching the spectrometer. There was a lot of background IR emission “noise” from the hot graphite walls and plasma. Also, any large unreacted particles of carbon travelling in the path of the emitted IR signal would scatter the signal from reaching the spectrometer. Nonetheless, fullerene emission was detected on the reactor. This achievement was the first of its kind ever described. To have a device that can directly detect the real-time production of fullerenes *in situ* in an operating reactor is ground breaking. Not only can this help develop new methods to make fullerenes, but also enhance these methods by detecting if impurities are formed.

Real-time spectroscopic measurements using OES on the reactor was also performed. These spectra yielded very useful information. The spectrometer measured the Swan Band region of the EM spectrum. Emission signals corresponding to carbon dimers and CN radicals were detected on the operating reactor. By investigating each emission signal more deeply, information regarding the relative concentrations of each species, and residence time were determined. From these experiments, it was found that OES can successfully track the presence of impurities, effects on yield and provide details of reaction chemistry and mechanisms, therefore, confirming the previous hypotheses.

From what has been discovered from this project, it can confidently be said that the use of spectroscopy as a detector of fullerenes is valid. On an operating reactor, it can determine the presence of fullerenes. However, to quantitate the exact concentration of fullerene molecules proved to be a challenge. One change that could help make the emission signal of fullerenes more reliable is an increase of the volume of the reactor and plasma. This would allow for a higher residence time of the carbon in the plasma, which would lead to greater evaporation. The more evaporation of the carbon would result in smaller or no unreacted carbon particles aerosols, which could potentially block the viewport. Design changes could be made on the reactor to incorporate a much larger viewport. A larger viewport would allow for measurements at different points in the reaction zone. Also, the detector used for this study was a single channel detector. This means that the detector could only view one wavelength at a time. Essentially, the spectrometer was taking limited narrow snapshots of the reaction zone. A multi-channel detector would allow for a sweeping scan would could be over a narrow range of a single broad peak and capture any shifts or broadening. Alternatively, multiple areas of the electromagnetic spectrum could be viewed at once which would allow for more reliable data because the four active modes of C_{60} could be detected simultaneously, peak widths would be more apparent, and the intensities of the peaks would be more accurate as to what is going on inside the reactor. Finally, since the IR emission of fullerenes was successful on an off-line fullerene vapour sublimator, the use of spectroscopy on an on-line sublimator would be equally beneficial. In the sublimator, there would be no unreacted carbon particles interfering with the emission signal. Since the sublimator is on-line and indicative of the chemistry that occurring inside the reactor, this could serve as a detector and controller of fullerene production. Since the next step would be to make this a large-scale production of fullerenes, incorporating an on-line sublimator in this process seems to be the best option.

11.0 Future Work / Recommendation

To achieve a more reliable result using the IRS as a tool for fullerene detection, I recommend bypassing parts of with large amounts of interfering soot. This can be done by using an on-line sublimator to separate and recover the fullerenes from the soot. The team is already developing this and the IRS would cleanly detect fullerenes in the gas phase. In this region, there will be no signal interference from the soot crowding the field of view.

Since the fullerenes travelling through the sublimator would be the fullerenes made from the reactor, this will serve as an accurate representation of the fullerenes formed from plasma treatment of the feedstock. Through this method, calculating the fullerene content in the gas phase in real time could achieved and by relating to the feedstock rate an overall production yield (weight fullerene out / weight carbon in) could be determined.

A direct real-time sensor of fullerene yield would be powerful tool in reactor optimization as all possible parameters could be rapidly explored to generate a multi-dimensional yield map and discover a global maximum for yield, or where highest production rates can be realized.

Bibliography

(1) H. W. Kroto, J. R. Heath, S.C. O'Brien, R. F. Curl, R. E. S. C60: Buckminsterfullerene. *Nature* **1985**, *318*, 162–163.

(2) Krätschmer, W., Lamb, L. D., Fostiropoulos, K., and Huffmann, D. R. Solid C_{60}: A New Form of Carbon. *Nature* **1990**, No. 347, 354–358.

(3) Gains, R. E.; Outlook Brightens for Plastic Solar Cells. *Science News* [Online], April 15, **2011**, pp 293 http://science.sciencemag.org/content/332/6027/293.long*332* (accessed August 14, 2018).

(4) Chistyakov, V. A.; Smirnova, Y. O.; Prazdnova, E. V; Soldatov, A. V. Possible Mechanisms of Fullerene C_{60} Antioxidant Action. *Biomed Res. Int.* **2013**, *2013*, 1-4.

(5) D.G. Tochil'nikov, B. M. G. Influence of C_{60}-Containing Additives in Lubricant Oil on the Optimization of Processes in the Boundary Friction of Metals. *Tech. Phys.* **1999**, *6* (44), 700–703.

(6) Fullerene https://en.wikipedia.org/wiki/Fullerene (accessed Aug 14, 2018).

(7) Rodgers, P. Solar Power Viable Within A Decade, Says IEA. *Forbes* [Online], September 30, **2014**, https://www.forbes.com/sites/paulrodgers/2014/09/30/the-rise-of-solar/#76eb2f5857e5 (accededed August 14, 2018).

(8) Sunlight https://en.wikipedia.org/wiki/Sunlight (accessed Aug 14, 2018).

(9) Lalwani, G.; Sitharaman, B. Multifunctional Fullerene- and Metallofullerene-Based Nanobiomaterials. Nano LIFE. **2013**, 3 (3), 1–22.

(10) Green, D. Advantages and disadvantages of Solar Photovoltaic – Quick Pros and Cons of Solar PV. Renewable Energy World [Online], Dec 19, **2012**, https://www.renewableenergyworld.com/ugc/articles/2012/12/advantages-and-disadvantages-of-solar-photovoltaic--quick-pros-and-cons-of-solar-pv.html (accessed Sep 20, 2018).

(11) Gribov, B. G.; Zinov, K. V. Preparation of High-Purity Silicon for Solar Cells. **2003**, *39* (7), 653–662.

(12) Haufler, R. E.; Chai, Y.; Chibante, L. P. F.; Conceicao, J.; Jin, C.; Wang, L.-S.; Maruyama, S.; Smalley, R. E. Carbon Arc Generation of C_{60}. *Mat. Res. Soc. Symp. Proc.* **1991**, p 627.

(13) Fulcheri, L., Schwob, Y., Fabry, F., Flamant, G., Chibante, L. F. P, Laplaze, D. No Title. *Carbon N. Y.* **1999**, *38*, 797–803.

(14) Guillard, T.; Flamant, G.; Laplaze, D. Heat, Mass, and Fluid Flow in a Solar Reactor for Fullerene Synthesis. *J. Sol. Energy Eng.* **2001**, *123* (2), 153.

(15) Howard JB, McKinnon JT, Makarovsky Y, Lafleur AL, J. M. Fullerenes C_{60} and C_{70} in Flames. *Nature* **1991**, *352* (6331), 139–141.

(16) Loutfy, R. O.; Lowe, T. P.; Moravsky, A. P.; Katagiri, S. Commercial Production of Fullerenes and Carbon Nanotubes. *Perspect. Fuller. Nanotechnol.* **2002**, 35–46.

(17) Garde, S. Physical Chemistry: Hydrophobic Interactions in Context. *Nature* **2015**, *517*, 277–279.

(18) Christopher A. Hunter, J. K. M. S. The Nature of .Pi.-.Pi. Interactions. *J. Am. Chem. Soc.* **1990**, *14* (112), 5525–5534.

(19) Holstein, B. R. The van Der Waals Interaction. *Am. J. Phys.* **2001**, *69*, 441.

(20) Semenov, K. N.; Charykov, N. A.; Keskinov, V. A.; Piartman, A. K.; Blokhin, A. A.; Kopyrin, A. A. Solubility of Light Fullerenes in Organic Solvents. *J. Chem. Eng. Data* **2010**, *55* (1), 13–36.

(21) Fulcheri, L.; Fabry, F.; Rohani, V. The Influence of the Carbon Precursor, Carbon Feed Rate and Helium Gas Flow Rate on the Synthesis of Fullerenes from Carbon Powder in an Entrained Flow 3-Phase AC Plasma Reactor Operating at Atmospheric Pressure. *Carbon N. Y.* **2012**, *50* (12), 4524–4533.

(22) Connor, S. Why the world is running out of helium. *Independent* [Online], August 23, **2010**, https://www.independent.co.uk/news/science/why-the-world-is-running-out-of-helium-2059357.html (accessed Aug 15, 2018).

(23) Solution, D. of S. P. of a C. S. No Title. *J. Phys. Chem.* **1992**, *96*, 6752–6755.

(24) Periodic Table: Carbon.

(25) Gruenberger, T. M. Continuous Production of Fullerenes and Other Carbon Nanomaterials on a Semi-Industrial Scale Using Plasma Technology. *AIP Conf. Proc.* **2002**, *633* (2002), 7–11.

(26) Smalley, R. E. Self Assembly of Fullerenes. *Acc. Chem. Res.* **1992**, *25*, 98–105.

(27) A. Brockhinke, M. Letzgus, S. Rinne, K. K.-K. Energy Transfer in the D3Πg−a3Πu (0−0) Swan Bands of C_2: Implications for Quantitative Measurements. *J. Phys. Chem.* **2006**, *9* (110), 3028–3035.

(28) Frum, C. I.; Engleman, R.; Hedderich, H. G.; Bernath, P. F.; Lamb, L. D.; Huffman, D. R. The Infrared Emission Spectrum of Gas-Phase C_{60} (Buckmisterfullerene). *Chem. Phys. Lett.* **1991**, *176* (6), 504–508.

(29) Sellgren, K.; Werner, M. W.; Ingalls, J. G.; Smith, J. D. T.; Carleton, T. M.; Joblin, C. C60 in Reflection Nebulae. *Astrophys. J. Lett.* **2010**, *722* (1 PART 2), 54–57.

(30) Jan Cami, Jeronimo Bernard-Salas, Els Peeters, S. E. M. Detection of C_{60} and C_{70} a Young Planetary Nebula. *Science (80-.).* **2010**, *329*, 1180–1182.

(31) *Benzene anhydrous, 99.8%*; MSDS No. 71-43-2 [Online]; Sigma Aldrich: Oakville, ON, September 29, **2017**. https://www.sigmaaldrich.com/catalog/product/sial/401765?lang=en&region=CA (accessed Aug 15, 2018).

(32) *Toluene*; MSDS No. 108-88-3 [Online]; Sigma Aldrich: Oakville, ON, September 21, **2017**. https://www.sigmaaldrich.com/catalog/substance/toluene921410888311?lang=en&region=CA (accessed Aug 15, 2018).

(33) NPI (Nationalk Pollution Inventory). Emission Estimation Technique Manual. **2012**, No. February 1999, 1–89.

(34) Osler. Canadian Government Carbon and Greenhouse Gas Legislation https://www.osler.com/en/resources/regulations/2015/carbon-ghg/canadian-government-carbon-and-greenhouse-gas-legi (accessed Sep 29, 2018).

(35) MTR ltd. MTR Fullerene Products Price List http://www.mtr-ltd.com/PriceList.htm (accessed Aug 15, 2018).

(36) R . F . Curl and R . C . Smalley. On the Formation of the Fullerenes. *Physical Sciences and Engineering.* Vol . 343 , No . 1667

(37) Lee, J. H. Recycling Studies for the Production of Fullerenes. Masters Thesis, University of New Brunswick, Fredericton, NB, **2017**.

(38) Haufler, R. E.; Conceicao, J.; Chibante, L. P. F.; Chai, Y.; Byrne, N. E.; Flanagan, S.; Haley, M. M.; O'Brien, S. C.; Pan, C.; Xiao, Z.; et al. Efficient Production of C_{60} (Buckminsterfullerene), $C_{60}H_{36}$, and the Solvated Buckide Ion. *J. Phys. Chem.* **1990**, *94* (24), 8634–8636.

(39) Knudsen, M. Die Gesetze Der Molekularströmung Und Der Inneren Reibungsströmung Der Gase Durch Röhren. *Ann. Phys.* **1909**, *29*, 75–130.

(40) Anisa, I.; Morad, N. Effect of Extraction Time on Degradation of Bioactive Compounds (Zingiber Officinale Roscoe). *J. Teknol. Sciences Eng.* **2014**, *67* (4), 63–66.

(41) Ahrens, J.; Bachmann, M.; Baum, T.; Griesheimer, J.; Kovacs, R.; Weilmünster, P.; Homann, K. H. Fullerenes and Their Ions in Hydrocarbon Flames. *Int. J. Mass Spectrom. Ion Process.* **1994**, *138* (C), 133–148.

(42) Gruenberger, T. M. Continuous Production of Fullerenes and Other Carbon Nanomaterials on a Semi-Industrial Scale Using Plasma Technology. *AIP Conf. Proc.* **2002**, *633* (October 2002), 7–11.

(43) Rohlfing, E. A.; Cox, D. M.; Kaldor, A. J. Development and Application of Laser Methods for Electroic Spectroscopy of Radicals. *J. Chem. Phys.* **1984**, *81*, 3322–3333.

(44) Zimba, J. Cooling of an Ideal Gas by Rapid Expansion Evaporative Cooling of Microscopic Water Droplets in Vacuo: Molecular Dynamics Simulations and Kinetic Gas Theory Cooling of an Ideal Gas by Rapid Expansion. *Am. J. Phys. J.* **2006**, *7474* (73), 124502–124554.

(45) Yamaguchi, S. M. and Y. A Molecular Dynamics Demonstration of Annealing to a Perfect C_{60} Structure, *Chem Phys Lett* **1998,** 286(3) 343-349.

(46) Rohlfing, E. A. Optical Emission Studies of Atomic, Molecular, and Particulate Carbon Produced from a Laser Vaporization Cluster Source. *J. Chem. Phys.* **1988**, *89* (10), 6103–6112.

(47) Todorović-Marković, B.; Marković, Z.; Mohai, I.; Károly, Z.; Farkas, Z.; Nikolić, Z.; Szépvölgyi, J. Optical Diagnostics of Fullerene Synthesis in the RF Thermal

Plasma Process. *J. Serbian Chem. Soc.* **2005**, *70* (1), 79–85.

(48) Crc. Properties of Carrier Gases for Gas Chromatography. *Crc* **1994**, 843–843.

(49) Harris, Daniel C., and Michael D. Bertolucci. Symmetry and Spectroscopy: an Introduction to Vibrational and Electronic Spectroscopy. New York: Dover Publications, 1989. Print.

(50) Iglesias-Groth, S.; Cataldo, F.; Manchado, A. Infrared Spectroscopy and Integrated Molar Absorptivity of C_{60} and C_{70} Fullerenes at Extreme Temperatures. *Mon. Not. R. Astron. Soc.* **2011**, *413* (2010), 213–222.

(51) Technologies, A. LII 200 Laser - Induced Incandescence Instrument for Soot Characterization. Company Brochure **2013**

(52) HORIBA. Spectroscopy Solutions - Mid-Focal Length Imaging Spectrometer – iHR Series https://www.horiba.com/en_en/products/detail/action/show/Product/spectroscopy-solutions-mid-focal-length-imaging-spectrometer-ihr-series-1590/.

(53) Robbins, L.H., Farabaugh, E.N., Feldman, A. Growth of Diamond Films by Hot Filament Vapor Deposition. *J. Mater. Res. Technol.* **1990**, *5*, 2546.

(54) Hanson. Lecture 6: Spectral Lineshapes. Presented at Princeton University, Princeton, NJ.

(55) Bates, S. C. *Net Shape Bulk Diamond Fabrication*; Glastonbury. http://www.tvu.com/PC60diamWeb.html

Curriculum Vitae

Eric Fradsham

Universities Attended:

Bachelor of Science with Honours, Medicinal Chemistry 2015

- University of New Brunswick, Fredericton, N.B.
- Research Supervisor: Dr. S. McGrady
  Title of Project: Solid-State Structural and Electrostatic Potential Analysis of Ammonia Borane Derivatives

Master of Science, Chemical Engineering 2019

- University of New Brunswick, Fredericton, N.B.
- Research Supervisor: Dr. L. P. F. Chibante
- Title of Project: Novel Use of On-Line Diagnostics for the Improved Production of Fullerenes

Academic Awards and Achievements:

- Recipient of NBIF-STEM Scholarship, 2016-2017
- Canadian Association of Chemistry Certification, 2015

Publications:

- Supramolecular interactions in boron hydrides: how non-classical bonding directs their crystal architecture. McGrady, G. S., Fradsham, E., Wolstenholme, D. Crystal Engineering Communications. 2015
- Nanomaterial Production using High Temperature Plasma. Sarawagi, AR, Fradsham EJ, Lee JH, Chibante LPF. UNB Graduate Conference. 2017. (Poster)